A COMPREHENSIVE STUDY OF MODELING MULTIPHASE FLOW THROUGH CHOKES

A Thesis

by

TIANHANG ZHOU

Submitted to the Office of Graduate and Professional Studies of
Texas A&M University
in partial fulfillment of the requirements for the degree of

MASTER OF SCIENCE

Chair of Committee,	A. Rashid Hasan
Committee Members,	Eduardo Gildin
	Marcelo Sanchez
Head of Department,	A. Daniel Hill

August 2017

Major Subject: Petroleum Engineering

ABSTRACT

Choke is an essential device that controls flow rates at either subsurface or surface. Many models and correlations have appeared for handling multiphase flow through surface chokes. However, direct comparison of their relative performances hasn't been studied before, it is difficult to choose the right model or correlation for rate calculation. This thesis has evaluated and studied several models and correlations to explore their relative merits and ease of use in field settings. Seven different data sets gathered from laboratory and field, involving 1,004 independent data points, constituted the essence of this study. As expected, models anchored in thermodynamic principles outperformed others.

The performance of the slippage effect was also studied. Seven slip equations were studied to determine which slip correlation showed best performance. The study found the constants proposed by Simpson et al. used in Grolmes and Leung equation showed best performance for flow through chokes.

The study also found the importance of PVT data in flow through choke calculations. Specifically, changes in density and heat capacity with pressure and temperature should be part of any rigorous effort for flow rates computation. The rate-dependent choke discharge coefficient approach, generated from field data, outperforms the fixed discharge coefficient concept of existing models.

Based on the results, the Sachdeva and Brill model performed consistently well among those considered models. Two different approaches of modifications were offered:

first, replace the specific-heat capacity ratio k by polytropic-gas-expansion coefficient n. With the optimized discharge coefficient, the accuracy was not changed much but this modification was recommended from the theoretical aspect. Second, introduce a slippage factor. However, the results showed that slippage played a minor role in estimating flow rate. This conclusion was also supported by slip velocity and flow pattern calculated. The Sachdeva and Brill model without slippage factor turned out to outperform others.

Among the correlations studied, the Fortunati correlation showed best performance but still not as good as all other models. This correlation also distinguishes flow boundary and flow type, which is an issue for the application of Al-Attar and B-K correlation. The Ashford and Pierce correlation, originally developed for subcritical flow, handles choke size up to 20/64 in. Increasing choke size requires adjustment of the choke discharge coefficient, which leads to unreliable solutions. For B-K correlation and Al-Attar critical correlation, they both use empirical coefficients derived from a particular field, which makes the correlation unreliable for other applications. Both correlations show huge errors, and B-K correlation mainly overestimates results.

ACKNOWLEDGEMENTS

I would like to thank my committee chair, Professor A. Rashid Hasan at Texas A&M University, for directing my research during my graduate study. He has been helpful, and I really appreciate that he has always had his door open for me. In addition, I would also like to thank my committee members, Dr. Eduardo Gildin and Dr. Marcelo Sancez, for their guidance and support throughout the course of this research.

I would also like to express appreciation to Shah Kabir of University of Houston for helping me define the topic for my thesis, providing data set for study and giving me a lot of assistance and guidance along my study.

Thanks also go to my friends and colleagues and the department faculty and staff for making my time at Texas A&M University a great experience.

CONTRIBUTORS AND FUNDING SOURCES

Contributors

This work was supervised by a thesis (or) dissertation committee consisting of Professor A. Rashid. Hasan and Eduardo. Gildin of the Department of Petroleum Engineering and Professor Marcelo. Sanchez of the Department of Industrial Engineering.

The lab data from Rajesh. Sachdeva Thesis in Year 1984 was provided by Professor Cem. Sarica of The University of Tulsa.

Some of the field data was provided by Shah. Kabir of University of Houston.

All other work conducted for the thesis (or) dissertation was completed by the student independently under the advisement of A. Rashid. Hasan of the Department of Petroleum Engineering.

Funding Sources

There are no outside funding contributions to acknowledge related to the research and compilation of this document.

NOMENCLATURE

A	Area, ft^2
B_o	Oil formation volume factor, bbl/STB
C_d	Discharge Coefficient
C_L	Heat capacity for liquid, $\frac{ft-lbf}{lbm-R}$
C_p	Heat capacity at constant pressure for gas, $\frac{ft-lbf}{lbm-F}$
C_v	Heat capacity at constant volume for gas, $\frac{ft-lbf}{lbm-R}$
CV	Control volume
d	Diameter, ft
d_c	Choke or orifice diameter, 1/64 inch.
d_d	Pipe diameter downstream of the choke, ft
d_u	Pipe diameter upstream of the choke, ft
f	Volume fraction, dimensionless
g_c	Gravitational constant, $\frac{lbm-ft}{lbf-s^2}$
GLR	Producing Gas Liquid Ratio (GLR) at standard condition, scf/STB
k	Specific heat capacity ratio, C_p/C_v
M	Molar mass, $\frac{lbm}{lbm-mol}$
$\dot{m}$	Mass flow rate, $\frac{lbm}{s}$
n	Polytropic gas expansion coefficient, dimensionless

N	Total number of data
P	Pressure, psia
P_{wh}	Wellhead pressure, psia
P_b	Bubble point pressure, psia
Q_g	Gas volumetric flow rate, scf/day
Q_l	Liquid volumetric flow rate, STB/day
Q_o	Oil volumetric flow rate, STB/day
Q_m	Mixture volumetric flow rate, $\frac{ft^3}{day}$
$Q_{calculated}$	Calculated volumetric flow rate, STB/day
$Q_{measured}$	Measured volumetric flow rate, STB/day
R	Universal gas constant, $\frac{ft-lbf}{lbmmol-°R}$
R_p	Producing Gas Oil Ratio (GOR) at standard condition, scf/STB
R_s	Solution GOR, scf/STB
R_{sw}	Soluability of gas in water, scf/STB
S	Slip ratio
T	Temperature, °F or °R
v	Specific volume = $1/\rho$ ($\frac{ft^3}{lbm}$)
V	Velocity, $\frac{ft}{sec}$
F_{wo}	Water oil ratio (WOR), STB/STB
x	Mass quality, dimensionless
y	Downstream to upstream pressure ratio, dimensionless

y_g	Mole fraction of gas, dimensionless
Z	Gas compressibility factor, dimensionless
β	Gas concentration used in Fortunati correlation
ρ	Density, $\frac{\text{lbm}}{\text{ft}^3}$
γ	Gravity
γ_{oa}	Oil gravity, °API
ε_1	Average relative error
ε_2	Average absolute error
ε_3	Standard deviation

SUBSCRIPTS

1	Upstream choke conditions
2	Choke throat conditions
3	Conditions just downstream of the choke throat
4	Recovered condition downstream of polytropic compression
d	Downstream of choke
e	Momemtum
g	Gas phase
k	Kinetic
l	Liquid phase
o	Oil phase
w	Water phase
α	Void fraction

H	Homogeneous
wh	Well head condition

TABLE OF CONTENTS

Page

ABSTRACT ii

ACKNOWLEDGEMENTS iv

CONTRIBUTORS AND FUNDING SOURCES v

NOMENCLATURE vi

TABLE OF CONTENTS x

LIST OF FIGURES xiii

LIST OF TABLES xv

1 INTRODUCTION 1

1.1. Problem Description 3
1.2. Study Main Objective 3
1.3. Study Specific Objectives 3
1.4. Methodology 4

2 GENERAL THEORY AND LITERATURE REVIEW 6

2.1. Choke Flow Geometry Sketch and Description 6
2.2. Flow Regime: Critical Flow and Subcritical Flow 7
2.3. Multiphase Flow Through Choke and Basic Principles Used 9
2.4. The Slippage Effect and Slip Ratio 11
2.5. The Slip Velocity 14
2.6. Density Integrated Average 14
2.7. Model Calibration and the Discharge Coefficient 16

3 EXISTING MULTIPHASE FLOW MODELS 18

3.1. Sachdeva et al. Model 18
3.2. Perkins Model 20
3.3. Al-Safran and Kelkar Model 26

4 EXISTING MULTIPHASE FLOW CORRELATIONS 29

4.1. Fortunati Correlation 29
4.2. Ashford and Pierce Correlation 34

4.3. Al-Attar Correlation 38
4.4. Beiranvand and Khorzoughi (B-K) Correlation 41

5 INTRODUCTION OF DATA SET STUDIED 43

5.1. Lab Data Set Introduction 43
5.2. Field Data Set Introduction 43

6 RESULTS 46

6.1. Evaluation Criteria 46
6.2. Discharge Coefficient Value Optimization 47
6.3. Models Evaluated 48
6.3.1. Sachdeva et al. Model 48
6.3.2. Sachdeva et al. Model with k/n Correction 49
6.3.3. Perkins Model 51
6.3.4. Al-Safran and Kelkar Model 52
6.3.5. Sachdeva et al. Model with Slip and k/n Correction 54
6.3.6. Discharge Coefficient 60
6.4. Correlation Results 63
6.4.1. Fortunati Correlation 63
6.4.2. Ashford and Pierce Correlation 65
6.4.3. Al-Attar Correlation 69
6.4.4. B-K Correlation 71

7 DISCUSSIONS 73

7.1. Evaluated Models Discussion 73
7.1.1. Sachdeva et al. Model 73
7.1.2. Sachdeva et al. Model with k/n Correction 73
7.1.3. Perkins Model 73
7.1.4. Kelkar Model 74
7.1.5. Sachdeva et al. Model with Slip (Simpson et al.) 75
7.1.6. Overall Discussions on Models Evaluated 75
7.1.7. Discussion on Slippage Effect 78
7.2. Evaluated Correlations Discussions 80
7.2.1. Fortunati Correlation 80
7.2.2. Ashford and Pierce Correlation 80
7.2.3. Al-Attar Correlation 81
7.2.4. B-K Correlation 82
7.2.5. Overall Discussion for Correlations 82

8 CONCLUSIONS 84

8.1. Conclusions 84

8.2. Future Work 85

REFERENCES 86

APPENDIX A 89

APPENDIX B 92

APPENDIX C 93

APPENDIX D 95

APPENDIX E 96

LIST OF FIGURES

Page

Figure 2-1: Diagram of Choke and Choke Flow Geometry 6

Figure 4-1: Velocity of Gas-Oil Mixtures Through Chokes (Fortunati, 1972) 31

Figure 6-1: Lab Data Results of Sachdeva et al. Model (1986) (Cd=0.845) 48

Figure 6-2: Field Data Results of Sachdeva et al. Model (1986) (Cd=0.83) 49

Figure 6-3: Lab Data Results of Sachdeva et al. Model with k/n Correction (Cd=0.90) 50

Figure 6-4: Field Data Results of Sachdeva et al. Model with k/n Correction (Cd=0.90) 51

Figure 6-5: Lab Data Results of Perkins Model (1993) (Cd=0.89) 51

Figure 6-6: Field Data Results of Perkins Model (1993) (Cd=0.905) 52

Figure 6-7: Lab Data Results of Al-Safran and Kelkar Model (2007) (Cd=0.62) 53

Figure 6-8: Field Data Results of Al-Safran and Kelkar Model (2007) (Cd=0.75) 54

Figure 6-9: Lab Data Results for 7 Slip Equations Used on Sachdeva et al. Model 55

Figure 6-10: Field Data Results for 7 Slip Equations Used on Sachdeva et al. Model 55

Figure 6-11: Lab Data Results of Sachdeva Model with Slip (Simpson et al.) (Cd=0.66) 56

Figure 6-12: Field Data Results of Sachdeva Model with Slip (Simpson et al.) (Cd=0.752) 57

Figure 6-13: Slip Velocity Results for Lab Data 58

Figure 6-14: Slip Velocity Results for Field Data 59

Figure 6-15: Discharge Coefficient for Lab Data 61

Figure 6-16: Discharge Coefficient for Field Data 62

Figure 6-17: Lab Data Results of Fortunati Correlation (1972) (Cd=0.81) 64

Figure 6-18: Field Data Results of Fortunati Correlation (1972) (Cd=1.08) 65

Figure 6-19: Discharge Coefficient Values for Ashford and Pierce Correlation (1975) .67
Figure 6-20: Lab Data Results of Ashford and Pierce Correlation (1975) (Cd=0.72).....68
Figure 6-21: Field Data Results of Ashford and Pierce Correlation (1975) (Cd=0.53)...69
Figure 6-22: Lab Data Results of Al-Attar Correlation (2010).....70
Figure 6-23: Field Data Results of Al-Attar Correlation (2010).....70
Figure 6-24: Lab Data Results of B-K Correlation (2012) 71
Figure 6-25: Field Data Results of B-K Correlation (2012) 72
Figure 7-1: Lab Performance Comparison for All Models Studied.....77
Figure 7-2: Lab Performance Comparison for All Models Studied.....77
Figure 7-3: Lab Performance Comparison for Correlations Studied 83
Figure 7-4: Field Performance Comparison for Correlations Studied 83

LIST OF TABLES

Page

Table 2-1: Constant Values for Grolmes and Leung Slip Correlation (Grolmes and Leung, 1985).....13

Table 4-1: Empirical Coefficients of Al-Attar Critical Flow (Al-Attar, 2009).....39

Table 6-1: Statistical Results for Lab Slip Velocity.....59

Table 6-2: Statistical Results for Field Slip Velocity.....60

Table 6-3: Observed and Calculated Cd Values for Ashford and Pierce Correlation.....66

Table 7-1: Lab Data Error Compared to Sachdeva et al. Model with k/n Correction 76

Table 7-2: Field Data Error Compared to Sachdeva et al. Model with k/n Correction....76

1 INTRODUCTION

A choke restricts fluid flow by incorporating an orifice to control flow rate or downstream pipe pressure drop. Choke or orifice is widely used in the oil and gas industry for controlling and optimizing production flow rates. In addition, choke is also able to provide backpressure for reservoir so that formation damage, large pressure fluctuations, and back-flow problems can be minimized.

It is commonly a critical parameter to measure the flow rate of fluids, either single phase flow or multiphase flow. This is because knowing flow rates can not only help predict potential performances of the wells and reservoir but also help make accurate determination for further economic and performance enhancement activity decisions. Even though there are a series of liquid and gas flow measurement instruments, the cost could be expensive and the problem that how to accurately measure flow rate of fluids especially oil-gas-water mixtures in such dynamic underground situations remains one of the key challenges in the petroleum industry. The variations of flow rate across choke can determine pressure drop. Hence, by measuring the pressure drop through choke flow rate of fluids may be determined indirectly.

Many models and correlations have been developed to determine flow rates through choke in the industry. However, with the different types of chokes, choke geometry could be extremely complicated. The flow pattern of flow entering the choke is also difficult to predict because it is not homogeneous flow any more but instead may be annular flow, bubbly flow, stratified flow, etc. The prediction for transition between critical and

subcritical flow is also significant because flow performances for these two conditions can vary a lot which will be demonstrated later in the theory part. Therefore, a small variation in the upstream condition of choke may cause much larger than expected deviations in flow rate predictions. It is important to evaluate different models and correlations and find their relative accuracy and stability.

Different models and correlations that utilize measured pressure drop across the choke to predict mass flow rate for multiphase flow through chokes are studied. Descriptions of models and correlations are shown in CHAPTER 3. The evaluation results for models and correlations are shown in CHAPTER 5. An improvement on prediction accuracy is also proposed by introducing an empirical equation of discharge coefficient which is used as a final modifying factor in the flow rate equation based on Reynold's number. The focus on models will be Sachdeva model (1986) because this model has shown the best performance in this study. Considering work that has been conducted on Sachdeva model (1986) previously suggested that there are areas could be further improved. Accordingly, two different modifications are presented.

There are total 7 different data sets that will be further described in CHAPTER 4. These data sets are then sub-divided into 5 field data sets and 2 lab data sets. Behaviors of multiphase flow for field conditions can be very different from theoretical lab conditions. Because eventually purpose of modeling is to serve for actual fields, it is hence important to study modeling performances and possible improvements based on field data set. By evaluating over 1,000 data points, results show that slip effect doesn't improves prediction accuracy for flow rate. Therefore, the slip ratio equations currently used in the industry

discussed in CHAPTER 2.4 are studied to determine which slip correlation shows most accurate performance for critical and subcritical flow individually. The mathematical derivation of Sachdeva model with slip ratio and k/n correction is shown in APPENDIX D.

1.1. Problem Description

A series of Models and correlations studied for multiphase flow through chokes have been developed. Models are complicated to calculate but can determine flow boundary and mass flow rate with more stable accuracy. Most correlations are not able to determine flow boundary but they are easier to apply. Hence, each model and correlation has unique advantages and disadvantages. However, a comprehensive study about what extent of relative stability and accuracy of each model and correlation can achieve based on a series of reliable data set instead of a particular field data set is rare in the industry.

1.2. Study Main Objective

The main objective of this thesis is to evaluate different models and correlations that utilize measured pressure drop across the choke to predict mass flow rate for multiphase flow through chokes.

1.3. Study Specific Objectives

i. To study and evaluate existing multiphase flow through chokes models and correlations widely used in the industry;
ii. Apply two modifications on Sachdeva et al. (1986) multiphase flow through chokes model;

iii. To generate a generate correlation for discharge coefficient based on Reynold's number.

1.4. Methodology

First, literature reviews were conducted to have a comprehensive understanding of problem and areas need to be improved. There are totally four main different areas that literature reviews are conducted which are shown in the following:

i. Density integration for multiphase flow and mass/momentum/energy conservation during multiphase flow through chokes;
ii. Fluid flow through chokes and corresponding pressure drop;
iii. Existing models and correlations for multiphase flow through chokes;
iv. The slippage effect of multiphase flow and slip ratio;

Then selected existing models, correlations and slip correlations are then studied to determine the model or correlation that gives best prediction relative stability and accuracy. Two modifications on Sachdeva et al. model (1986) are conducted to correct one theoretical mistake and see if the model can be further improved. Before generating results, all selected models and correlations are tested by using the same data set the original author utilized when introducing their model or correlation. Until the results of average error, average absolute error and standard deviation match with those generated by the original author, the evaluation of models and correlations on data set of this thesis study can be continued. The slip velocity and flow pattern were calculated to further investigate slippage effect.

Lastly, a general correlation for discharge coefficient which is used to correct final mass flow rate and absorb modeling errors is generated based on Reynolds number.

2 GENERAL THEORY AND LITERATURE REVIEW

2.1. Choke Flow Geometry Sketch and Description

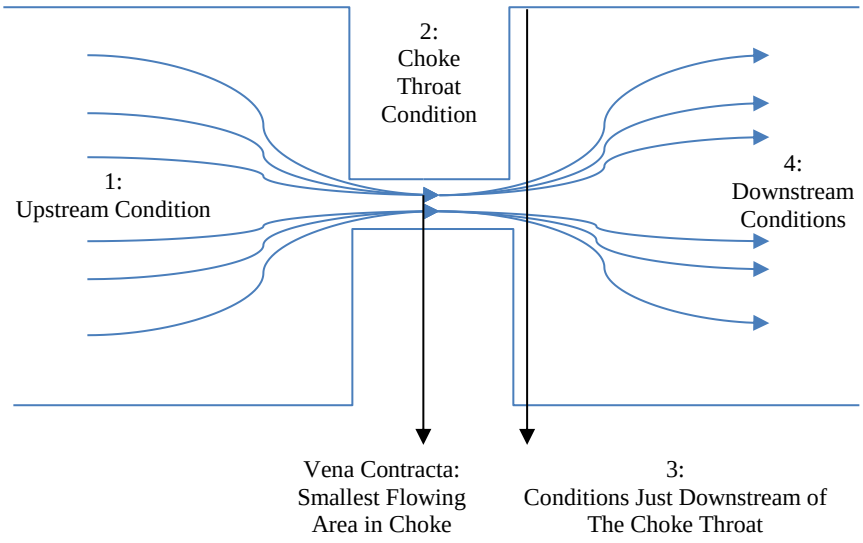

Figure 2-1: Diagram of Choke and Choke Flow Geometry

Figure 2-1 shows a simplified sketch of choke and choke flow geometry. There are totally four important flow conditions in choke modeling which are labeled out in the figure. The distances between these four conditions are chosen arbitrarily. Condition 1 represents the upstream condition, where the inlet parameters, such as upstream pressure/temperature/velocity are measured. The choke throat condition is represented by condition 2, where the flow is accelerated and pressure drop occurs. The reason why condition 3 where the flow is separated after choke throat and encountered an abrupt area enlargement is shown particularly is because the just downstream position of choke throat is important for subcritical flow. When subcritical flow occurs, this position needs to be considered for accurate prediction. Condition 4 indicates downstream position, where the fluid flow exactly reaches the pipe wall and have homogeneous velocity again. Because

there is no direct contact between fluid and pipe wall the friction effect is assumed to be negligible from condition 3 to 4. The outlet parameters, such as downstream pressure/temperature/velocity are measured at this position.

Schuller et al. 2003 introduced an idea of vena contracta which is the smallest flowing area point of choke. The entrances of most choke geometries will make fluids encounter a sudden contraction. Fluid flow will become much more turbulent through chokes and hence it is not possible for fluids to utilize the entire choke internal area. There will be one particular point that the choke areas utilized by fluids will reach minimum, this point is called vena contracta. The fluid flow velocity reaches maximum at the vena contracta point.

When modeling choke multiphase flow, it is assumed that flow from condition 1 to 4 is adiabatic. In addition, the flow is assumed to disperse sufficiently to neglect any variation between gas, oil and water phases. Hence, from condition 1 to 4 all phases are assumed to have same temperature. Besides temperature, the mass quality of all phases is assumed to stay constant from previous studies.

2.2. Flow Regime: Critical Flow and Subcritical Flow

There are total three different flow regimes may occur during fluid flow through chokes: critical, subcritical and supercritical flow. However, for supersonic flow, the fluid velocity is even higher than the local speed of sound, which seldom happens in oil and gas producing systems. Hence, the supercritical flow regime is not studied.

The critical flow occurs when the fluid velocity reaches exactly same as the velocity of sound in the same medium when fluid flows through the smallest area of choke and

reaches a maximum value. Variations in pressures between upstream and downstream will induce pressure waves, which then propagate through the flow from downstream to upstream and consequently affect flow rate and upstream pressure. However, if the fluid velocity is higher than the velocity of pressure waves the waves are no longer able to propagate to upstream. Hence, any pressure variation or reduction in the downstream will not have any effect on flow rate; flow rate will be an independent variable of downstream pressure until the critical/subcritical flow boundary is reached. Under this circumstance, the upstream pressure will not be affected. (Sachdeva et al., 1986). Predicting flow rate for critical flow condition is preferable because upstream condition is relatively stable and the critical flow rate can be calculated the maximum flow rate through chokes, which many processes are saved.

Nevertheless, when the fluid velocity fails to reach velocity of sound in the same medium when fluid flows through the smallest area of choke, in other words, downstream pressure is beyond the flow boundary point, subcritical flow dominates. Compared to critical flow, subcritical flow rate depends on the pressure differential across choke and the pressure waves caused by downstream pressure fluctuations will affect upstream pressure. (Al-Safran and Kelkar, 2009). The prediction processes for critical and subcritical flow can vary a lot so it is very important to calculate the flow boundary accurately.

Even though flow rate is independent of downstream pressure for critical flow, the variation of upstream parameters still has effect on flow rate. Sachdeva et al. (1986) showed that the critical flow rate mostly has a direct proportion with fluid density. By

increasing upstream pressure will cause liquid density increasing and hence giving a larger critical mass flow rate. If increasing temperature, gas density will decrease and then reduce fluid critical mass flow rate. However, the contribution of gas density to the whole fluid density is relatively small compared to liquid phase, so variations in liquid density tends to show larger effect on critical mass flow rate.

Lastly, because of the relatively high density of liquid phase and compressibility of gas phase. Elastic waves tend to occur for multiphase flow which propagate slower than shock waves. Consequently, the critical flow regime is easier to reach for multiphase flow than single-phase flow because speed of sound in multiphase flow will be lower than single-phase flow. On the other hand, requirement of flow boundary for multiphase flow with identical other variables as single-phase tends to be higher than single-phase flow.

2.3. Multiphase Flow Through Choke and Basic Principles Used

A wellhead choke is usually used to control well production rate and pressure drop so that the fluctuations in the downstream of choke have no effect on the production rate. To take such effects, choke installed in the pipe or tubing of producing wells reduces local flowing area and hence cause the acceleration of fluid flow. Based on Bernoulli's Law, if there is a fluid speed acceleration occurred, there must be a simultaneously fluid potential energy decreasing or pressure drop. Because the length of choke is relatively short the potential energy change is assumed to be negligible during this process. Therefore, a pressure drop must occur in this situation. A simple form of Bernoulli equation can be derived for steady and incompressible flow which is shown in Equation (1) and Equation (2):

$$p + \rho\frac{V^2}{2} = \text{constant} \tag{1}$$

$$\frac{dp}{dV} + \rho V dV = 0 \tag{2}$$

When modeling multiphase flow, there are three conservation laws commonly used as basic principles: law of conservation of mass, law of conservation of momentum and law of conservation of energy.

i. Law of conservation of mass: mass flows in must equal to mass flows out: $\dot{m}_{in} = \dot{m}_{out}$ or $\frac{d}{dx}\dot{m} = 0$. Then the relationship between volumetric flow rate of fluids which is the target for prediction and flowing area, velocity and density can be derived, which is shown in Equation Set. (3):

$$\dot{m}_{in} = \dot{m}_{out}$$

$$\rho_{in}A_{in}V_{in}\Delta t = \rho_{out}A_{out}V_{out}\Delta t$$

$$Q_{in\_i}\rho_{in\_i} = \rho_{in\_i}A_{in\_i}V_{in\_i} = \rho_{out\_i}A_{out\_i}V_{out\_i} = Q_{out\_i}\rho_{out\_i} \tag{3}$$

ii. Law of conservation of momentum: the total momentum before a collision of two objects is equal to total momentum after a collision. The original momentum conservation equation can be seen in Equation (4):

$$\frac{Adp_4}{dz} = \frac{d\left(V_4\dot{m}_{l,4} + V_4\dot{m}_{g,4}\right)}{dz} \tag{4}$$

If generating relationship between mass flow rate and flow velocity from Equation (5):

$$V_4 = \frac{\dot{m}_4}{\rho_e A} \tag{5}$$

Then substitute Equation (5) into Equation (4), the final momentum conservation Equation (6) is achieved:

$$A\frac{dp_4}{dz} = \frac{d}{dz}\left(\frac{\dot{m}_4^2}{\rho_e A}\right) \tag{6}$$

The momentum density: ρ_e is used in the momentum conservation Equation

iii. Law of conservation of energy: Energy can neither be created nor destroyed but can only be transformed from one object to another. The principle is shown in Equation (7):

$$\frac{d}{dz}\left(h_m + \frac{\dot{m}_4^2}{2\rho_k^2 A^2} + \frac{\rho_m}{\rho_k} g\sin\theta z\right) = \text{heat flux} \tag{7}$$

in which h_m represents mixture enthalpy, the kinetic energy density ρ_k is used.

2.4. The Slippage Effect and Slip Ratio

Slippage effect is a commonly mentioned parameter for fluid flow in control volume. For single-phase gas flow, the Klinkenberg slippage effect has been used for years. For liquid-gas multiphase flow, the slippage effect resulted from velocity difference between gas and liquid phase velocities and may influence the pressure drop and mass flow rate through chokes. Among the plentiful models and correlations developed to predict mass flow rate through chokes, most of them skip including slippage effect because either investigations on slippage effect haven't been conducted extensive enough the time correlation or model is developed or the author holds the opinion that slippage effect won't affect prediction performance much. Among all models widely accepted in the industry, only the Hydro model developed by Shuller et al. (2003) and Al-Safran and Kelkar Model (2009) include slippage effect.

Equation **(**8**)** shows a universally acknowledged expression for slip ratio S, also known as velocity ratio, which is used to account slippage effect:

$$S = \frac{V_g}{V_l} \tag{8}$$

For gas, oil and water three-phase flow, because water and oil are usually assumed to have similar properties compared to gas, the velocity of oil phase and water phase are then assumed to be the same and hence constitute a liquid phase. As can be seen, if gas velocity is also identical with liquid phase, the slip ratio will be equal to 1 which means there is no slippage effect. However, only when gas quality is relatively low or homogeneous flow can this no-slip phenomenon be achieved. Normally gas flows much faster than liquid and even faster with higher gas quality, leading to slip ratio bigger than unity value.

Though the general equation for slip ratio is present, it is difficult to accurately measure flow velocity of gas phase and liquid phase individually when flowing through chokes. Flow velocity of gas phase is normally extremely high when flowing through restrictions so expressions which are more convenient to use are required.

Grolmes and Leung (1985) introduced a general slip correlation, which is shown in Equation (9):

$$S = a_0 \left(\frac{1 - x_g}{x_g}\right)^{a_1 - 1} \left(\frac{\rho_l}{\rho_g}\right)^{a_2 + 1} \left(\frac{\mu_l}{\mu_g}\right)^{a_3} \tag{9}$$

The applicable values of constants a_0, a_1, a_2, a_3 are shown in Table 2-1. There are totally 8 different slip correlations derived from the general correlation if considering the homogeneous equation with no slip. These correlations are studied all together with a new

Hydro Slip Correlation developed by R. B. Schuller et al. (2003). Results of performances of these slip correlations are shown in the results section.

Table 2-1: Constant Values for Grolmes and Leung Slip Correlation (Grolmes and Leung, 1985)

Correlation	a_0	a_1	a_2	a_3
Homogeneous (no slip)	1	1	-1	0
Constant Slip	Slip Ratio (S)	1	-1	0
Fauske	1	1	-1/2	0
Moody	1	1	-2/3	0
Simpson et al.	1	1	-5/6	0
Thom	1	1	0.89	0.18
Baroczy	1	0.74	0.65	0.13
Lockhart-Martinelli	0.28	0.64	0.36	0.07

Based on experimental results, Schuller et al. (2003) developed a new slip correlation for the Hydro Model, which is shown in Equation (10).

$$S = \sqrt{1 + x_g\left(\frac{\rho_l}{\rho_g} - 1\right)}\left[1 + \xi e^{-\beta x_g}\right] \tag{10}$$

The modification for this slip correlation correct the Grolmes and Leung slip correlation when gas quality is low. The constant values of ξ and β were recommended to be 0.6 and 5.0.

2.5. The Slip Velocity

When gas phase rises through liquid phase, there is a difference between average velocities of different mixture phases. This difference is referenced as slip velocity which is shown in Equation (11). Because slippage effect can't be statistically calculated directly, slippage velocity is frequently used as an evaluation standard on the existence of slippage effect. If slippage velocity is relatively negligible compared to interfacial gas velocity, then a conclusion that the slippage effect is also negligible could be made. Kabir and Hasan (2004) studied performance of no-slip homogeneous model for gas/condensate wells and presented that the homogeneous model without any slip is as good as any other sophisticated model and when annular/mist flow occurs there is no slip appearing during the entire process. For annular/mist flow, high gas velocities occur and tend to carry liquid phase, there is little relative motion between the phases and slippage effect is negligible for such situations.

$$V_{slip} = V_g - V_l = \frac{V_{superficial,g}}{f_g} - \frac{V_{superficial,l}}{f_l} \tag{11}$$

2.6. Density Integrated Average

When dealing with multiphase flow, one of the reasons that it is more complicated than single phase flow is because for different phases, properties such as density, velocity and viscosity may vary a lot. This variation is more significant between gas and liquid phase. Therefore, these properties need to be interpreted as integrated average values. If both water and oil phase are present simultaneously, it is common to treat these two phases as liquid phase and then utilized to interpret average values together with gas phase.

Among the properties that needs to be interpreted as integrated averages for different phases, density is an important parameter which critical flow velocity mostly depends on. Hence, it is significant to apply a distinction between different densities at different positions for different phases. This is because the contribution of each phase may be considered differently. R. B. Schuller (2003) showed that there are generally 3 different ways which contribution of phases can be weighed into integrated density values. First, if the mass in a control volume dominates, the corresponding density is called mixture density, which is represented by: ρ_m (specific volume: v_m) and shown in Equation (12), which slip effect is considered and an additional slip ratio factor is included.

$$v_m = \frac{1}{\rho_m} = \frac{\frac{x_g}{\rho_g} + S\frac{(1-x_g)}{\rho_l}}{x_g + S(1-x_g)} \tag{12}$$

If the density is based on the net momentum flux through control volume and hence the surface force dominates, then the density is called momentum density: ρ_e (specific volume v_e) and shown in Equation (13) including slip ratio.

$$v_e = \frac{1}{\rho_e} = \left[\frac{x_g}{\rho_g} + S\frac{(1-x_g)}{\rho_l}\right]\left[x_g + \frac{1-x_g}{S}\right] \tag{13}$$

If there is no slip effect considered, then slip ratio S=1, both momentum and mixture density can be simplified into homogeneous density, which is shown in Equation (14):

$$v_H = \frac{1}{\rho_H} = \frac{1}{x_g\rho_g + (1-x_g)\rho_l} \tag{14}$$

R. B. Shuller (2003) introduced a fourth density equation which is called kinetic energy density: ρ_k (specific volume: v_k) and shown in Equation (15).

$$v_k = \frac{1}{\rho_k} = \left[\frac{x_g}{\rho_g} + S\frac{(1-x_g)}{\rho_l}\right]\sqrt{x_g\frac{(1-x_g)}{S^2}} \quad (15)$$

However, because for choke multiphase flow modeling, homogeneous density and momentum density are mostly used, the explanation and derivation of kinetic energy density will not be included in this thesis.

Among the density equations, Chisholm. D (1983) stated that if elevation variation is the main reason of pressure drop then the mixture density equation should be applied and momentum density is most suitable in modeling where fluid acceleration causes pressure drop through chokes. Because the elevation change through chokes is negligible, momentum density is preferable in modeling choke multiphase flow than mixture density. If there is no slippage effect considered in modeling, the momentum density is then simplified to homogeneous density. For momentum density and homogeneous density, based on over 1,000 data points evaluated, momentum density tends to always be higher than homogeneous density.

2.7. Model Calibration and the Discharge Coefficient

The discharge coefficient, also known as Cd, is normally used to calibrate and improve prediction accuracy for multiphase flow through chokes models and correlations. A "perfect" model is supposed to have a unity discharge coefficient. However, it is not possible to perfectly model multiphase flow behavior through a restriction such as choke. This is because no matter how accurate the modeling is, there must exist some levels of errors depending on what assumptions are made and how much extent of accuracy is sacrificed. The discharge coefficient is then selected to adsorb such errors induced. Almost

every commonly used correlation or model has their unique discharge constant values. This is because normally a discharge coefficient value is derived from the results calculated from the study. Study approaches, assumptions made and even the data set used for different models and correlations are not the same and may vary a lot.

When calculating the discharge coefficient, there are generally two most commonly used approaches. One method is to find a value which leads to minimum error, the least square method is normally used for this approach. Then this particular value is used as a constant to calibrate prediction results. This method has some disadvantages because the data set evaluated are usually limited while there are many kinds of field conditions in the industry. Therefore, the Cd value needs to be calibrated and adjusted each time for different field conditions. In addition, while the error is minimized, standard deviation which is another important evaluation factor may also be compromised. Another method is to derive a general equation of Cd based on Reynolds number, choke configuration, and fluid properties. There are also literatures shown to plot Cd values against production rate measured for simplicity. A best-fit line needs to be made through the data points and the corresponding trendline will be used as a general equation for Cd values. If the data points are broad enough, the equation derived could be used as a general industry guideline for the formation or reservoir studied.

3 EXISTING MULTIPHASE FLOW MODELS

This study evaluates three models and two modifications conducted on one of the models for predicting mass flow rate of multiphase mixture flow through a choke that are most commonly used in the current oil and gas industry. The models studied are Sachdeva et al. model (1986), Perkins model (1993) and the Al-Safran and Kelkar model (2007). As can be seen, the models studied are spread from 1980s to 2010s, which ensure the diversity of models. All models chosen are widely accepted in the industry. Some relatively old models such as Sachdeva et al. model and Perkins model are still widely used in the current industry. All models could determine critical and subcritical flow boundary.

As demonstrated earlier by Al-Safran and Kelkar (2009), they recommended two modifications for Sachdeva model. These modifications were also tested in this research to see the relative accuracy and stability. Firstly, by replacing the specific-heat capacity ratio: k by polytropic-gas-expansion coefficient: n. Secondly, by introducing a slippage factor using the Schuller (2006) slip correlation for critical flow, and the Grolmes and Leung (1985) slip correlation for subcritical flow.

3.1. Sachdeva et al. Model

Sachdeva, Brill, Schmidt and Blais developed a multiphase flow model though chokes for predicting mass flow rate and flow boundary in 1986. The motivation of their study was because majority correlations were only applicable for critical flow while subcritical flow was also vital for most wells and inaccurate prediction will contribute to poor performances of entire production system analysis. Based on the principal of mass, momentum and energy conservation, the model can calculate flow boundary and mass

flow rate for both critical and subcritical flow regimes. (R. Sachdeva et al. 1986). An expression for the highest pressure ratio that will give critical point was developed. R. Sachdeva et al. (1986) made the following assumptions during developing the model:

a) Flow is one dimensional;

b) Phase velocities are equal at the throat;

c) The predominant term of pressure drop is flow acceleration;

d) Flow is "frozen", quality is constant for entire process;

e) The liquid phase is incompressible.

Lab experiments were conducted to gather data for critical flow, subcritical flow and flow on boundary. Kerosene, air and water were used as three mediums to simulate multiphase flow. Air-water and air-kerosene flow data were gathered for five different choke diameters and three flow regimes. The total six different sets of data were computed by using the model and then results were compared with empirical data achieved from lab experiments.

The following Equation (16) shows how Sachdeva et al. (1986) calculated critical and subcritical flow boundary:

$$y_c = \left\{ \frac{\frac{k}{k-1} + \frac{1 - x_l V_l (1-y)}{x_l V_l}}{\frac{k}{k-1} + \frac{n}{2} + \frac{n(1-x_l)v_l}{x_l v_{G4}} + \frac{n}{2}\left[\frac{(1-x_l)v}{x_l v_{G4}}\right]^2} \right\}^{\frac{k}{k-1}} \tag{16}$$

where Equation (17) shows expression of polytropic-gas-expansion coefficient n:

$$n = 1 + \left(\frac{x_l (C_p - C_v)}{x_l C_v + (1 - x_l) C_L} \right) \tag{17}$$

When the phase composition is pure gas phase, the critical pressure ratio can be derived by the following simplified Equation (18):

$$y_c = \left(\frac{2}{k+1}\right)^{\frac{k}{k-1}} \tag{18}$$

Critical flow exists when the value of $y_{actual} < y_c$ and subcritical flow occurs when the value of $y_{actual} > y_c$. If $y_{actual} = y_c$, then flow is at the flow boundary.

Once the critical-subcritical pressure boundary is determined, the following Equation (19) is used to calculate flow rates through the choke:

$$\dot{m}_4 = C_D \left\{ 2g_c \times 144 P_1 \rho_{m4}^2 \left[\frac{(1-x_l)(1-y)}{\rho_l} + \frac{x_l k}{k-1} (v_{G1} - y v_{G4}) \right] \right\}^{0.5} \tag{19}$$

where the homogeneous density equation is used which is shown in Equation (20) and the downstream gas specific volume can be written as an equation of upstream gas specific volume, as shown in Equation (21):

$$\frac{1}{\rho_{m4}} = x_l V_{G4} + (1-x_l) V_L \tag{20}$$

$$V_{G4} = V_{G1} y^{-\frac{1}{k}} \tag{21}$$

Average error rate and standard deviation showed that this model outperformed other correlations and models. It was recommended to utilize this model only when ratio of choke size to pipe diameter is no more than 0.5 and a discharge coefficient of 0.85 should be used to account for error correction (Sachdeva et al. 1986).

3.2. Perkins Model

Thomas K. Perkins, 1993 derived a mathematical equation including mass and energy conservation principle for determining critical and subcritical flow boundary. In his

approach, Perkins (1993) proposed correlations of reduced gas compressibility, oil and water properties. A total of 1431 data sets are analyzed to output the optimal value of discharge coefficient. The best discharge coefficient found is 0.826, yielding a 15.41% standard deviation and 11.46% mean absolute error.

To develop the model for multiphase flow through restrictions, Perkins (1993) made following assumptions:

a) The flow is isentropic flow (adiabatic with no friction);
b) The flow is one dimension direction;
c) At any point of multiphase flow through chokes, all phases have constant temperature;
d) At any point of multiphase flow through chokes, all phases have same velocity;
e) Gas phase has a constant compressibility factor;
f) Liquid phase is incompressible compared to gas phase;
g) The elevation change of choke area is negligible.

Critical and subcritical flow boundary is determined by using following Equation (22):

$$\left[2\lambda\left(1-p_r^{\frac{n-1}{n}}\right)+2\alpha_1(1-p_r)\right]$$
$$\left\{\left[1-\left(\frac{A_4}{A_1}\right)^2\left(\frac{f_g+\alpha_1}{f_g p_r^{-\frac{1}{n}}+\alpha_1}\right)^2\right]\left[\frac{f_g}{n}p_r^{-\frac{1+n}{n}}\right]+\left(\frac{A_4}{A_1}\right)^2\frac{f_g}{n}\frac{\left(f_g+\alpha_1\right)^2 p_r^{-\frac{(1+n)}{n}}}{\left(f_g p_r^{-\frac{1}{n}}+\alpha_1\right)^2}\right\} \quad (22)$$

$$= \left[1 - \left(\frac{A_4}{A_1}\right)\left(\frac{f_g + \alpha_1}{f_g p_r^{-\frac{1}{n}} + \alpha_1}\right)^2\right]\left(f_g p_r^{-\frac{1}{n}} + \alpha_1\right) \times [\lambda\left(\frac{n-1}{n}\right) p_r^{-\frac{1}{n}} + \alpha_1$$

where, the expression of λ, n and α_1 can be found in Equation (23), Equation (24) and Equation (25):

$$\lambda = \left(f_g + \frac{\left(f_g C_{vg} + f_o C_{vo} + f_w C_{vw}\right)M}{zR}\right) \tag{23}$$

$$n = \frac{k f_g C_{vg} + f_o C_{vo} + f_w C_{vw}}{f_g C_{vg} + f_o C_{vo} + f_w C_{vw}} \tag{24}$$

$$\alpha_1 = \frac{1}{v_1}\left(\frac{f_o}{\rho_o} + \frac{f_w}{\rho_w}\right) \tag{25}$$

To calculate the mass flow rate, Perkins (1993) proposed an approach to determine the boundary between critical flow and subcritical flow first. The mass flow rate through restriction is calculated by applying the following steps:

i. Iterate pressure ratio p_r from in Equation (22) until the equation converges, the corresponding p_r is the flow boundary. For each pressure ratio iterated, re-calculate P_2, T_2 and use the average pressure and temperature to determine corresponding properties by the following Equation (26), Equation (27), Equation (28) and Equation (29):

$$p_2 = p_r \times p_1 \tag{26}$$

$$T_2 + 460 = (T_1 + 460) p_r^{\frac{n-1}{n}} \tag{27}$$

$$p_{avg} = \frac{p_1 + p_2}{2} \tag{28}$$

$$T_{avg} = \frac{(T_1 + T_2)}{2} \tag{29}$$

ii. With the final p_r from iteration, solve for p_2 again, and use following Equation (30) to solve for p_3 (the pressure just downstream of the choke throat) by using the Perry relationship for subcritical flow:

$$p_3 = p_1 - \frac{p_1 - p_2}{\left[1 - \left(\frac{d_c}{d_p}\right)^{1.85}\right]} \tag{30}$$

iii. To determine if the flow is critical or subcritical, utilize the following criteria:

If $p_2 > p_3$ critical flow exists and the p_r value calculated from iteration above should be used for mass flow rate determination;

If $p_2 < p_3$, flow is subcritical flow, use the actual $p_r = \frac{p_3}{p_1}$ to calculate corresponding mass flow rate;

If $p_2 = p_3$, the flow is right at the critical and subcritical boundary, either $p_r = \frac{p_2}{p_1}$ or $p_r = \frac{p_3}{p_1}$ can be used.

Perkins (1993) then proposed a formula to calculate flowing fluid velocity by using the following Equation (31):

$$V_4 = \sqrt{\frac{288 g_c \{\lambda p_1 v_1 \left[1 - p_r^{\frac{n-1}{n}}\right] + \left[\left(\frac{f_o}{\rho_o}\right) + \left(\frac{f_w}{\rho_w}\right)\right] p_1 (1 - p_r)\}}{1 - \left(\frac{A_2}{A_1}\right)^2 \left[\frac{f_g + \alpha_1}{f_g p_r^{-\frac{1}{n}} + \alpha_1}\right]^2}} \tag{31}$$

The value 288 used in above equation was used as conversion factor. The value of p_r used is based on flow regime. Final mass flow rate is then calculated by using Equation (32):

$$\dot{m}_i = A_4\rho_4V_4 = \frac{A_4V_4}{[f_gv_4 + \left(\frac{f_o}{\rho_o}\right) + \left(\frac{f_w}{\rho_w}\right)]} \tag{32}$$

If substituting Equation (31) into Equation (32), a final form of mass flow rate is shown in Equation (33):

$$\dot{m}_i = A_4\sqrt{\frac{288g_cp_1/v_1\{\lambda\left[1 - p_r^{\frac{n-1}{n}}\right] + \alpha_1(1-p_r)\}}{\left[1 - \left(\frac{A_4}{A_1}\right)^2\left[\frac{f_g + \alpha_1}{f_gp_r^{-\frac{1}{n}} + \alpha_1}\right]^2\right]\left(f_gp_r^{-\frac{1}{n}} + \alpha_1\right)^2}} \tag{33}$$

Though above equation can yield mass flow rate, Perkins (1993) suggested that there should be another derivation for calculating the maximum possible flow rate. This process is finished by determining value of p_r which yields $\frac{d\dot{m}_i}{dp_r} = 0$, this value of p_r is the same value as p_r determined by Equation (34):

$$\frac{d}{dp_r}\left(\frac{\dot{m}_i}{A_4\sqrt{\frac{288g_cp_1}{v_1}}}\right)^2 = 0 \tag{34}$$

Perkins (1993) didn't include further details about how to solve Equation (34) step by step. Following steps show the mathematical derivation of solving corresponding p_r for maximum possible flow rate: After substituting mass flow rate formula, the following final derivation of p_r value is given in Equation (35):

$$\frac{d}{dp_r}\left(\frac{\left\{\lambda\left[1-p_r^{\frac{n-1}{n}}\right]+\alpha_1(1-p_r)\right\}}{\left[1-\left(\frac{A_4}{A_1}\right)^2\left[\frac{f_g+\alpha_1}{f_g p_r^{-\frac{1}{n}}+\alpha_1}\right]^2\right]\left(f_g p_r^{-\frac{1}{n}}+\alpha_1\right)^2}\right)=0 \tag{35}$$

By following the law of division derivation, final derivation is shown in Equation (36):

$$\frac{\begin{aligned}&\left\{\left[\lambda\frac{n-1}{n}\left(-p_r^{-\frac{1}{n}}\right)-\alpha_1\right]\left[\left(f_g p_r^{-\frac{1}{n}}+\alpha_1\right)^2-\left(\frac{A_4}{A_1}\right)^2(f_g+\alpha_1)^2\right]\right.\\&\left.-\left\{\lambda\left[1-p_r^{\frac{n-1}{n}}\right]+\alpha_1(1-p_r)\right\}\left[\left(-\frac{2}{n}\right)\left(f_g^2 p_r^{-\frac{3}{n}}+f_g p_r^{-\frac{2}{n}}\alpha_1\right)\right]\right\}\end{aligned}}{\left[\left(f_g p_r^{-\frac{1}{n}}+\alpha_1\right)^2-\left(\frac{A_4}{A_1}\right)^2(f_g+\alpha_1)^2\right]^2} \tag{36}$$

If equaling this derivation to 0, obviously the denominator can't be 0, so the nominator has to equal to 0. Hence, Equation (37) is proposed to iterate on p_r until left side of equation equals to right side.

$$\begin{aligned}&\left[\lambda\frac{n-1}{n}\left(-p_r^{-\frac{1}{n}}\right)-\alpha_1\right]\left[\left(f_g p_r^{-\frac{1}{n}}+\alpha_1\right)^2-\left(\frac{A_4}{A_1}\right)^2(f_g+\alpha_1)^2\right]\\&=\left\{\lambda\left[1-p_r^{\frac{n-1}{n}}\right]+\alpha_1(1-p_r)\right\}\left[\left(-\frac{2}{n}\right)\left(f_g^2 p_r^{-\frac{3}{n}}+f_g p_r^{-\frac{2}{n}}\alpha_1\right)\right]\end{aligned} \tag{37}$$

A programming language can be used to solve by creating a function which represents the left side of above expression and another function represents the right hand side of above expression, then use solve of excel to find the p_r value that yields LHS=RHS.

3.3. Al-Safran and Kelkar Model

Based on Sachdeva et al. model (1986) and Perkins model (1993), Al-Safran and Kelkar (2009) developed a model where the mathematical derivations and assumptions are very similar to Sachdeva et al. model (1986). The novelty part compared with Sachdeva et al. model (1993) is to include a pressure recovery just downstream of choke throat which comes from Perkins model (1993) and an additional slip ratio. The slip ratio generated from the Hydro model developed by Schuller et al. (2003) is used for critical flow, subcritical flow evaluation uses slip ratio from The Grolmes and Leung (1985) slip correlation.

The flow boundary is determined by using following Equation (38):

$$(y_c)^{1-\frac{1}{n}} = \frac{\alpha(1-y_c)+\frac{n}{n-1}}{\frac{n}{n-1}+\frac{n}{2}\left(1+\alpha y_c^{\frac{1}{n}}\right)^2} \tag{38}$$

where expressions of n and α are shown in Equation (39) and Equation (40):

$$n = \frac{x_g k C_{vg} + (1-x_g) C_l}{x_g C_{vg} + (1-x_g) C_l} \tag{39}$$

$$\alpha = \frac{S(1-x_g) v_l}{x_g v_{g1}} \tag{40}$$

The flow boundary y_c is found by iterating until Equation (38) is fulfilled. Al-Safran and Kelkar (2009) then proposed expression for calculating the critical and subcritical mass flow rate which is shown as Equation (41):

$$\dot{m}_i = \frac{C * A_4^2 p_1 [\alpha(1-y) + \frac{n}{n-1}\left(1 - y^{\frac{n-1}{n}}\right)]}{x_g v_{g1} \left(y^{-\frac{1}{n}} + \alpha\right)^2 [x_g + \frac{1}{S}(1-x_g)]} \quad (41)$$

in which, Al-Safran and Kelkar (2009) defined C as a constant which depends on unit system used. For customary units, the value of C was suggested to be ($C = 2C_D^2 g_c \times 144$). For SI units, C was originally suggested to be ($C = 2000C_D^2$). However, during evaluation of the model, it was found out correct value of C for SI units should be ($C = 2C_D^2$). This error was corrected for modeling in this study.

If actual choke throat pressure/upstream pressure ratio $\frac{p_2}{p_1}$ is smaller than critical pressure ratio y_c, then flow regime is critical flow and y_c should be used in Equation (41) to evaluate mass flow rate; If $\frac{p_2}{p_1}$ is larger than y_c, then flow regime is subcritical flow and the actual value of $\frac{p_2}{p_1}$ should be used. The variable p_2 which is the choke throat pressure is usually not measured because conditions at particular choke throat condition can be complicated and difficult to measure accurately. To estimate p_2, Al-Safran and Kelkar (2009) used approach proposed by Perkins (1993). First the pressure just downstream of choke p_3 is related to downstream pressure p_4 by using Equation (30). In the case of boundary flow, $p_2 = p_3$, p_2 is related to p_3 which can be calculated from measured downstream pressure.

A data set with total 57 data points was evaluated by Al-Safran and Kelkar (2009), which included 29 points acquired from Middle East fields and 28 data from Ashford and Pierce (1975). The results generated outperform both Sachdeva model (1986) and Perkins model (1993). The discharge coefficient, C_D is found to be 0.7 to 0.75.

Lastly, there is a mystery existing when determining flow boundary. Different slip ratio correlations were recommended for critical and subcritical flow. The equation used to determine flow boundary includes a slip ratio term. However, it is unknown which slip correlation should be used before the flow boundary value yc is calculated out. An example implementation is shown in APPENDIX C about how this issue is solved in this study.

4 EXISTING MULTIPHASE FLOW CORRELATIONS

This study evaluates four correlations for predicting mass flow rate of multiphase mixture flow through a choke that are most commonly used in the current oil and gas industry. The correlations studied are Fortunati correlation (1972), Ashford and Pierce correlation (1975), Al-Attar correlation (2010) and Beiranvand and Khorzoughi correlation (2011) (B-K correlation). As can be seen, the correlations studied are spread from 1970s to 2010s, which ensure the diversity of correlations studied. Among the correlations, the correlations can differentiate between critical and subcritical flow boundary are the Fortunati correlation and Ashford and Pierce correlation while B-K correlation could still be used without inputting flow boundary information. Al-Attar correlation would even need to input corresponding flow boundary information to compute as different approaches were proposed for critical and subcritical flow.

4.1. Fortunati Correlation

Fortunati (1972) developed a correlation to work for both critical and subcritical flow because during the 1970s most papers are only able to concern critical flow. The novelty of Fortunati correlation is not the fact that subcritical flow can be calculated with his correlation but the correlation can distinguish the critical and subcritical flow boundary. Though the approach proposed is complicated compared to existing models, Fortunati correlation is the only correlation able to determine flow boundary among the four correlations studied.

Similar as Perkins model (1993), Fortunati (1972) proposed formulas for calculating properties which are then used as intermediate parameters to calculate flow boundary and

mass flow rate. First, Fortunati (1972) made an assumption that oil flow rate at standard condition is equal to 1 STO cm^3. By using oil formation volume factor (FVF) and solution GOR at downstream condition, corresponding gas flow rate with assumed oil flow rate at standard condition could be calculated. Then gas concentration in Equation (42) was calculated by using the assumed oil rate and calculated gas rate. The mixture density then can be calculated as shown in Equation (43):

$$\beta = \frac{q_g}{q_g + q_o + q_w} = \frac{q_g^o \times B_g}{q_g B_g + q_o B_o + q_w B_w} \tag{42}$$

$$\rho_{mixture} = \frac{1-\beta}{B_o}(\rho_o^o + \rho_g^o R_{si}) \tag{43}$$

where the superscript o represents standard condition in Fortunati correlation. The solution GOR, oil FVF and gas FVF are evaluated at downstream condition.

Different from the three models discussed above, Fortunati (1972) proposed two different approaches for critical and subcritical flow rate estimation. The approach for critical flow rate is straight forward and is shown in Equation (44):

$$q_o^o = \frac{p_4 A_2}{\sqrt{(R_{si} - R_{s,4})(\rho_o^o + \rho_g^o R_{si})\frac{p_o Z T_4}{T^o}}} \tag{44}$$

It is important to mention that above expression is only valid for critical flow. To calculate the subcritical flow rate, the approach becomes much more complicated which needs to utilize information from Figure. 4-1. The experimental curves shown in the figure is plotted by using a 0.137 $\frac{MN}{M^2}$ (1,396 $\frac{Kg}{cm^2}$) choke downstream pressure. This figure is also used by Fortunati to determine critical and subcritical flow boundary. The shaded area

within the left and right boundary represents subcritical flow area. The remaining area outside of the boundary represents critical flow area. The downstream/upstream pressure ratio and mixture velocity (m/sec) are on the x-axis and y-axis respectively.

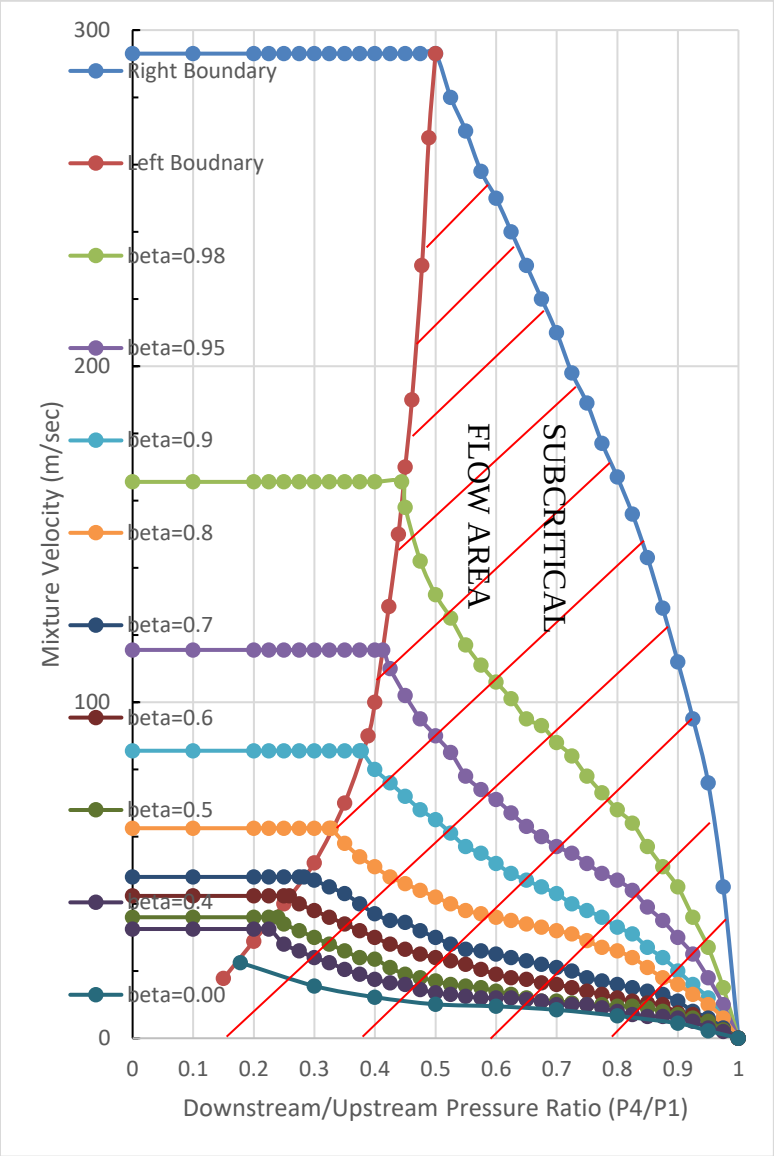

Figure 4-1: Velocity of Gas-Oil Mixtures Through Chokes (Fortunati, 1972)

To determine where the flow boundary is, it is necessary to either generate expressions for each boundary line and lines for different gas concentration values or for every data point read directly from the figure where the intersection of pressure ratio and mixture velocity is pointed to. Apparently, it is not practical to read from the figure manually. Therefore, besides existing points on the boundary and different gas concentration value lines provided by Fortunati (1972), more data points are read from the original figure and have been plotted into Figure 4-1 and used to generate expressions. The total data points used to plot the figure and expressions for different gas concentration values and boundary lines are shown in APPENDIX. E.

The actual P4/P1 pressure ratio can be easily calculated as both upstream and downstream pressure are measured and given as input parameters. However, to calculate the apparent mixture velocity which is shown in Equation (46), the mixture or phase velocity corresponding to the actual downstream pressure needs to be calculated first as shown in Equation (45):

$$V_{p_4} = \sqrt{\frac{np_4}{\beta \rho_{mixture}}} \tag{45}$$

$$V_{p4'} = \frac{V_{p_4}}{\left(\sqrt{\frac{p_4}{p_4'}}\right)^k} \tag{46}$$

where the variable p_4 represents the actual choke downstream pressure, p_4' represents the downstream pressure used which is $0.137\frac{MN}{M^2}$. The variable V_{p_4} and $V_{p4'}$ represent mixture or phase velocity corresponding to actual downstream pressure and the pressure

assumption $0.137\frac{MN}{M^2}$. The variable k in Equation (46) doesn't represent specific heat capacity any more but is an exponent which is shown in Equation (47):

$$K = (1 - \beta^3)^{0.38} \tag{47}$$

After the variable $V_{p4'}$ is calculated, together with the actual downstream/upstream pressure ratio, an intersection could be found on Figure 4-1, if this intersection is located in the subcritical flow area, then flow is subcritical; if this intersection is located in the critical flow area, then flow is critical flow. Because this study has a practical aim and the flow boundary determination approach is fully programmed in VBA which can be found in APPENDIX. E. By using programming tool, the P4/P1 pressure ratio on the left and right boundary of subcritical flow area can be found by inputting mixture velocity value at $0.137\frac{MN}{M^2}$ calculated from Equation (46). Then the actual P4/P1 pressure ratio is compared with left and right boundary P4/P1 pressure ratio values. If the calculated values is between left and right boundaries, then flow is subcritical; if not flow is critical.

The method for calculating critical flow rate is shown above. If the flow regime is subcritical, the following approaches should be used: based on the actual gas concentration and P4/P1 pressure ratio, the subcritical apparent velocity can be determined from Figure 4-1. In this study programming language is used to minimize errors caused from reading values on figure. Then Equation (46) is used again to calculate the true flow velocity, but this time $V_{p_4'}$ is known and V_{p_4} is to be calculated. This V_{p_4} value is the final subcritical flow rate.

4.2. Ashford and Pierce Correlation

F. E. Ashford and P. E. Pierce, in 1975 developed a correlation specifically used for describing multiphase flow and pressure drop through down-hole safety valves and the correlation was tested against field data with assumptions made. Ashford and Pierce (1975) pointed out that the correlation contains an improved formula for liquid flowing that considers solution gas and free gas. In addition, the correlation can determine critical and subcritical flow regimes. The corresponding critical and subcritical flow are handled by relating pressure drop through restrictions to flow rates and fluid properties. Ashford introduced an approach for calculating critical flow rate for multiphase flow in 1974. This work is an extension which includes both critical and subcritical flow correlations. Ashford and Pierce (1975) utilized concept of energy balance conservation which is shown in Equation (48):

$$144\int_{p_1}^{p_4} v_f = -\int_{V_1}^{V_4} \frac{V dV}{g_c} \tag{48}$$

This equation describes relationship between pressure volume energy loss and kinetic energy gain across the choke.

The final form of Ashford and Pierce correlation flow rate equation calculates oil flow rate directly. However, if there is no oil phase but instead gas and water phases this equation cannot be applied directly. In such situation, Equation (49) should be used to calculate downstream fluid velocity which is amenable to gas phase and one or more liquid phases present.

$$V_4 = \sqrt{\left(\frac{2k}{k-1}\right) g_c \left(\frac{1}{\rho_1} - \frac{1}{\rho_l}\right) p_1 \left(1 - y^{\frac{k-1}{k}}\right) + 2g_c \left(\frac{1}{\rho_l}\right) p_1 (1-y)} \tag{49}$$

Because mass flow rate though chokes can be written as a function of discharge coefficient, choke area, downstream fluid velocity and downstream fluid specific volume as shown in Equation (50):

$$\dot{m} = \frac{C_d A_c V_4}{v_{f4}} \tag{50}$$

If assuming liquid as incompressible phase, downstream gas specific volume can be expressed by using liquid specific volume and pressure ratio. Hence, downstream specific volume can be written as shown in Equation (51):

$$v_{f4} = v_l + v_{g1}\left(\frac{p_1}{p_4}\right)^{\frac{1}{k}} = v_l + (v_{f1} - v_l)\left(\frac{p_1}{p_4}\right)^{\frac{1}{k}} \tag{51}$$

By substituting Equation (51) and (49) into Equation (50), an initial form of flow rate can be derived and shown in Equation (52):

$$q = \frac{\dot{m}}{C_d A_c}\left(\frac{v_l}{2p_1 g_c}\right)^{0.5} = \frac{\left\{\frac{kR}{k-1}\left[1 - \left(\frac{p_4}{p_1}\right)^{\frac{k-1}{k}}\right] + \left(1 - \frac{p_4}{p_1}\right)\right\}^{0.5}}{1 + R\left(\frac{p_4}{p_1}\right)^{-\frac{1}{k}}} \tag{52}$$

Because the critical flow condition occurs with maximum flow rate simultaneously, by differentiating flow rate q in Equation (52) with respect to pressure ratio: y can yield an expression for determining flow boundary, which is shown in Equation (53):

$$1 = \frac{R_1/k\left[\left(\frac{R}{b}\right)\left(1 - y_c^b\right) + (1 - y_c)\right]}{0.5\left(1 + Ry_c^{-\frac{1}{k}}\right)^2 y_c^e} \tag{53}$$

in which, formulas of variables b and e can be found in Equation (54) and Equation (55):

$$b = \frac{k - 1}{k} \tag{54}$$

$$e = \frac{k + 1}{k} \tag{55}$$

If placing y_c on the left of equation and then rearrange Equation (53) to have a better view, Equation (56) is achieved:

$$y_c = \frac{R/k\left[R\left(\frac{k}{k-1}\right)\left(1 - y_c^{\frac{k-1}{k}}\right) + (1 - y_c)\right]}{0.5\left(1 + Ry_c^{-\frac{1}{k}}\right)^2 y_c^{\frac{1}{k}}} \tag{56}$$

To solve for critical and subcritical flow boundary: y_c, an iteration method needs to be used until either Equation (53) or (56) are fulfilled.

The variable R in Equation (53) and Equation (56) represents in-situ GLR, which can be calculated by using following Equation (57):

$$R(p, T) = \frac{p_{sc} T_1 Z_1}{p_1 T_{sc}} (R - R_{sl})\left(\frac{1}{5.615}\right) \tag{57}$$

where R represents producing GLR and R_{sl} represents solution GLR at upstream condition. Equations. (58) and (59) show how to calculate these two variables:

$$R = GOR_p(1 - F_{wo}) \tag{58}$$

$$R_{sl} = R_{so}(1 - F_{wo}) + R_{sw}F_{wo} \tag{59}$$

As mentioned, Ashford and Pierce (1975) developed a novel expression for liquid specific volume which uses solution GLR to replace total producing GLR and is shown in Equation (60):

$$v_l = \frac{B_o + F_{wo}}{\rho_o + \frac{R_s\rho_g}{5.615} + \rho_w F_{wo}} \tag{60}$$

If including the gas phase specific volume and relate mass flow rate to volumetric flow rate by using total fluid specific volume. Equation (61) Is achieved:

$$\dot{m}v_t = \dot{m}\frac{B_o + \left(\frac{R - R_s}{5.615}\right)\left(\frac{p_{sc}}{p_1}\right)\left(\frac{T_1 Z_1}{T_{sc}}\right) + F_{wo}}{\rho_o + \frac{R_s\rho_g}{5.615} + \rho_w F_{wo}} = q_t\left(\frac{5.615}{86{,}400}\right) \tag{61}$$

where the total fluid volumetric flow rate can be written as Equation (63):

$$q_t = q_o + q_g + q_w = q_o\left[B_o + \left(\frac{R - R_s}{5.615}\right)\left(\frac{p_{sc}}{p_1}\right)\left(\frac{T_1 Z_1}{T_{sc}}\right) + F_{wo}\right] \tag{62}$$

By substituting Equation (60), Equation (61) and Equation (62)(63) into Equation (52). The final expression for oil flow rate calculation results in Equation (63):

$$q_o = 3.51 C_d D_c^2 \alpha_{10}\beta_{10} \tag{63}$$

where the expressions of α_{10} and β_{10} are shown as follows in Equation (64) and (65):

$$\alpha_{10} = \frac{1}{\sqrt{B_o + F_{wo}}} \tag{64}$$

$$\beta_{10} = \frac{[\left(\frac{k}{k-1}\right) T_1 Z_1 (R_p - R_s)(1 - y^{\frac{k-1}{k}} + 198.6 p_1 (1 - y)]}{[198.6 + \frac{T_1 Z_1}{p_1}\left(R_p - R_s\right) y^{-\frac{1}{k}}]} \times \frac{\sqrt{\gamma_o + 0.000217\gamma_g R_s + F_{wo}\gamma_w}}{[\gamma_o + 0.000217\gamma_g R_p + F_{wo}\gamma_w]} \quad (65)$$

A field data with total 11 data points were used to test the correlation. Ashford and Pierce made following assumptions when using the field data set: WOR is assumed to equal to 1%; gas gravity, oil gravity, choke temperature and specific heat capacity are assumed to be 0.6, 0.85, 150 °F and 1.275 respectively. Based on results generated, an expression of discharge coefficient based on choke diameter was also proposed. However, because the data set only has a limited size, the expression is only valid for choke diameters ranged from 14/64th inch to 20/64th inch.

Al-Attar (2009) studied performances of Ashford and Pierce correlation and proposed discharge coefficient values for three additional choke diameters: 64, 96 and 144/64th inch. The values for these three choke diameters are 0.8108, 0.6964 and 0.4677 respectively.

4.3. Al-Attar Correlation

H. Al-Attar, in 2009 developed a correlation for critical and subcritical multiphase flow through chokes. Al-Attar developed two empirical critical flow equations based on 40 field tests from a high-rate oil field in the Middle East, and developed subcritical correlations based on 139 field tests from the same field. For critical flow, Al-Attar (2010) compared performances of his two empirical equations with six published correlations: Gilbert (1954), Baxendell (1957), Ros (1959), Achong (1961), Poettmann and Beck

(1963), and Ashford (1974). For subcritical flow, Fortunati (1972) and Ashford and Pierce (1975) correlation were selected to compare with.

Al-Attar also introduced equations for properties calculations which won't be discussed here as the focus is on his performances on critical and subcritical multiphase flow. There are total 3 different choke diameters from the field tests he conducted for both critical and subcritical flow: 64/64th inch, 96/64th inch and 144/64th inch. In addition, there are also three different choke types he studied for both critical and subcritical flow: Cameron LD, Cameron F and Bean type. To calculate critical flow liquid rate, two empirical equations were proposed which are shown as Equation (66) and Equation (67):

$$Q_l = Ap_1(GLR - R_{s1})^B D_c^C \tag{66}$$

$$Q_l = Dp_1 GLR^E D_c^F \tag{67}$$

where A, B, C, D, E, F are empirical coefficients derived by fitting the curve to the 40 critical field data. Table 4-1 shows values of these coefficients.

Table 4-1: Empirical Coefficients of Al-Attar Critical Flow (Al-Attar, 2009)

Choke Type	A	B	C	D	E	F
Cameron LD	4.543E-3	0.04921	1.7523	1.262E-3	0.247	1.733
Cameron F	9.454E-5	0.7911	1.7358	1.801E-1	-0.64	1.972
Bean setting	2.03E-3	0.1493	1.837	2.18E-3	0.0897	1.879

The empirical equations for critical flow proposed by Al-Attar show relatively better performances compared to other six correlations. However, the equations are not very

practical because the equations are generated by fitting to the 40 field test data. This makes the equations limited to a special operational condition for that particular field. In addition, only three different choke diameters were studied which are relatively large choke diameters in the industry. These two equations have shown poor performances when evaluating with data set of other fields.

For subcritical flow, Al-Attar (2009) introduced a new correlation that explicitly calculates liquid flow rate. Steps are shown as follows:

i. Calculate values of downstream fluid properties (R_s, B_o, Z);

ii. Calculate downstream no-slip gas hold up λ_{g2} by using Equation (68):

$$\lambda_{g2} = \frac{\left[3.27E-7\left(\frac{Z_4 T_4}{p_4}\right)(R_{si}-R_{s4})\right]}{\left[3.27E-7\left(\frac{Z_4 T_4}{p_4}\right)(R_{si}-R_{s4})\right]+6.49E-5(B_{o4}+F_{wo})]} \quad (68)$$

iii. Calculate the parameter of $\left(\frac{p_4}{p_1}\right)^{1-\lambda_{g2}}$;

iv. Based on the choke diameter, determine value of downstream mixture flow rate Q_{m4} by either calculating from equations or reading from figures.

v. The final form of oil flow rate can be calculated from Equation (69):

$$Q_o = \frac{15387 Q_{m4}(1-\lambda_{g4})}{B_{o4}+F_{wo}} \quad (69)$$

Because the equations and figures proposed by Al-Attar for downstream mixture flow rate are not practical, the equations and figures are not shown here. Al-Attar (2009) only shew Q_{m4} equations and figures for the three different choke diameters based on 139 subcritical flow tests. For other diameters, it is not applicable to calculate Q_{m4} based on

equations given. Al-Attar subcritical correlation therefore shows relatively large error performances.

Lastly, Al-Attar correlation is not able to distinguish between critical and subcritical flow boundary. To calculate corresponding flow rates, user will have to input flow regime information before applying equations or correlations.

4.4. Beiranvand and Khorzoughi (B-K) Correlation

M. S. Beiranvand and M. B. Khorzoughi, in 2012 developed a very easy-to-use correlation for multiphase flow through chokes by using new incorporated parameters. The motivation of their work is because most correlations in the industry are not practical and are limited to specific conditions. Their study proposed an empirical equation which contains six input parameters and six empirical coefficients. The formula was claimed that it could be applied for different operational conditions for different kinds of fields. The correlation was tested against 182 data from field production tests and showed better accuracy performances compared to five other empirical correlations. The newly incorporated parameter used in this correlation is the Basic Sediments & Water (BS&W). The final form of oil flow rate is shown in Equation (70):

$$Q_o = A\frac{P_{wh}^{F} D_c^{B}\left(1-\frac{BS\&W}{100}\right)^{D}\left(\frac{T}{T_{sc}}\right)^{E}}{GLR^{C}} \tag{70}$$

The values of empirical coefficients A, B, C, D, E, F are 1, 1.5, 0.5, 0.1, 1 and -0.8 respectively. The advantages of this correlation are that it is the easiest correlation to use for calculating oil flow rate of multiphase flow and user are only required to gather data of the six input parameters. However, the simplicity also contributes to its shortcomings:

First, it can only calculate oil flow rate. It is not valid any more if the liquid phase is mainly water phase; Second, with only six input parameters, the correlation accuracy will highly rely on the accuracy of these six parameters. If any single parameter is acquired inaccurately, the results may vary a lot. Furthermore, this correlation was a simply empirical equation generated by fitting to the 182 field data points. By studying this correlation for data set from this thesis study, some data sets show large error and standard deviation results which is against the claim that B-K correlation is proposed for different operational conditions from different fields. Lastly, this correlation is not able to determine critical and subcritical flow boundary.

5 INTRODUCTION OF DATA SET STUDIED

There are total 1,004 data points studied in this thesis, which further includes 629 lab data points and 375 field data points.

5.1. Lab Data Set Introduction

There are totally two lab data set with 629 data points studied, which are lab data from R. Sachdeva Thesis (1984), R. B. Schuller et al. (2003) and R. B. Schuller et al (2006).

For Sachdeva lab data set, two phase flow tests were conducted for critical, subcritical and boundary flow for the following five choke diameters: 16, 20, 24, 28 and 32/64th inch. Sachdeva lab data set contains 562 data points in total. 223 of them are critical points, 220 are subcritical points and 110 points are generated for boundary flow.

For Schuller lab data set presented by Schuller et al. (2003), there are totally 87 data points. 67 generated for gas-water-oil multiphase flow; 5 points are for single gas phase flow; 5 points are for single oil phase flow and there are 15 points used for single water phase flow. The choke diameter studied was fixed at 28/64th inch. Because the purpose of this study is to evaluate multiphase flow, all single phase flow data are not included. Only the 67 multiphase flow data are evaluated.

5.2. Field Data Set Introduction

There are five field data set with 375 data points studied in this thesis. The field data set studied are from: Shah Kabir of Unviersity of Houston, R. K. Haug (2012), Beiranvand and Khorzoughi (2011), Al-Safran and Kelkar (2009) and Ashford and Pierce (1975).

For field data set provided by Shah Kabir, there are 39 data points in total. 8 of them are critical flow, 31 of them are subcritical flow. The choke diameters studied are very diversified ranged from 16 to 48/64th inch.

For Haug field data set, there are 87 data points studied in total. Information about flow regime is not given. The choke diameters for this data set are 32, 56 and 96/64th inch. Oil density, gas density, gas mass quality and oil mass quality are calculated and given as inputs. However, the upstream pressure and temperature for this data set are relatively much higher, the upstream pressure mostly stays around 2,700 psi and can reach 3,100 psia while temperate is given as a fixed value of 172 °F. That may be because this field is a North Sea offshore field.

For Beiranvand and Khorzoughi field data set, there are 182 data points in total. This data set has the following five choke diameters: 25.6, 30.72, 38.4, 46.08, 51.2, 56.32, 61.44 and 64/64th inch. Information about flow regime is not given for this data set. Studied fluid properties and field descriptions are given by Beiranvand and Khorzoughi (2012). The assumptions of gas gravity and oil gravity are made.

For Al-Safran and Kelkar field data set, there are totally 32 data points included. This data set has the following five choke diameters: 24, 28, 32, 48, 64 and 96/64th inch. Information about flow regime is not given. The assumptions of WOR and upstream temperature are made by Al-Safran and Kelkar (2009).

For Ashford and Pierce field data set, there are totally 35 data points included which are all subcritical flow. This data set has the following three choke diameters: 14, 16 and 20/64th inch. The assumptions of WOR, upstream temperature, oil gravity, gas gravity and

specific heat capacity are made by Ashford and Pierce (1975). Because of so many assumptions made and limited data points, this data set lacks reliability compared to other data set.

6 RESULTS

All models and correlations studied in this study described were programmed in VBA. In this section results of existing models and correlations and that of the new developed Sachdeva model tested with 7 different slip ratio correlations are presented. For each model and correlation presented, statistical results and graphical representations for lab and field data set are presented and discussed separately by using the evaluation criteria mentioned in previous section of this thesis.

6.1. Evaluation Criteria

All selected choke models, correlations and slip correlations are evaluated with average relative error, average absolute error and standard deviation, which are shown in Equation (**71**), Equation (**72**) and Equation (**73**) respectively:

$$\varepsilon_1 = (\frac{1}{N}\sum_{i=1}^{N}\frac{Q_{pre}-Q_{mea}}{Q_{meas}})\times 100\% \tag{71}$$

$$\varepsilon_2 = (\frac{1}{N}\sum_{i=1}^{N}|\frac{Q_{pre}-Q_{mea}}{Q_{meas}}|)\times 100\% \tag{72}$$

$$\varepsilon_3 = \sqrt{\frac{1}{N-1}\sum_{i=1}^{N}\left[\left(\frac{Q_{pre}-Q_{mea}}{Q_{meas}}\right)-\varepsilon_1\right]^2}\times 100\% \tag{73}$$

Above equations only show examples about how results are evaluated. Based on different data set, different parameters could be used: liquid total volumetric flow rate, oil volumetric flow rate and total mass flow rate.

The average relative error measures the relative difference between calculated and measured results. However, if the over-predictions and under-predictions are evenly

spaced but far from measured values, average relative error can approach zero and fails to represent actual error. Therefore, average absolute error and standard deviation are required. Absolute average error calculates the absolute value of each error before taking the average, ε_2 will only be low if the overall error is small. Standard deviation measures how calculated results are spread around the average relative error.

6.2. Discharge Coefficient Value Optimization

The discharge coefficient values used originally for models and correlations are usually generated based on limited number of data. Though Perkins model (1993) used over 1,000 data to generate discharge coefficient, other models and correlations mostly used less than 100 data points and the data used are mostly from the same experimental or field conditions. To investigate the ultimate performances, it is important to determine the optimized Cd value first.

The least square method was used to iterate Cd value until the square of relative error is minimized. In this way, the minimization of average absolute error was guaranteed. However, the standard deviation is also a significant parameter used for evaluation, the Cd value for each model and correlation was then manually changed around the Cd value achieved from least square method until the optimized performances are achieved. Both average absolute error and standard deviation will be compromised to some level but only in this way can satisfy both criteria.

6.3. Models Evaluated

6.3.1. Sachdeva et al. Model

6.3.1.1. Applied to Lab Data Set

Figure 6-1 shows figures of model performances based on 629 lab data for Sachdeva et al. Model (1986). Instead of the 0.75 discharge coefficient value proposed, the optimized Cd value was found to be 0.845. With this Cd value, Sachdeva model showed an average error of -8.68%, an average absolute error of 12.65% and standard deviation of 12.80%. For critical flow, the three evaluation criteria are -11.91%, 14.35% and 11.17% respectively. For subcritical flow, the three evaluation criteria are -4.27%, 10.32% and 13.55% respectively.

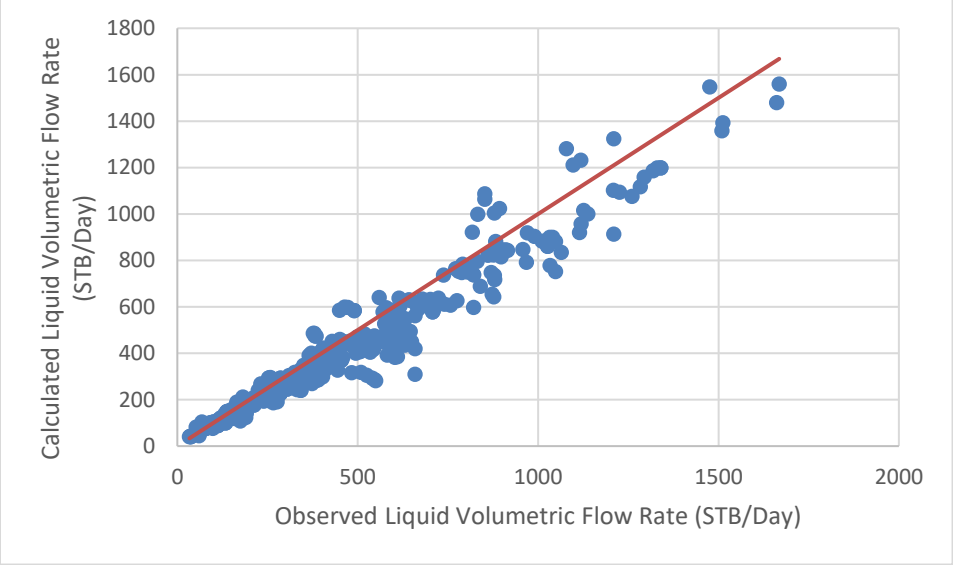

Figure 6-1: Lab Data Results of Sachdeva et al. Model (1986) (Cd=0.845)

6.3.1.2. Applied to Field Data Set

Figure 6-2 shows figures of model performances based on 375 field data for Sachdeva et al. Model (1986). The optimized Cd value was also found to be around 0.83. Sachdeva model showed an average error of -13.94%, an average absolute error of 22.26% and a standard deviation of 22.51%. For critical flow, the three evaluation criteria are -13.49%, 22.49% and 23.25% respectively. For subcritical flow, the three evaluation criteria are -16.43%, 20.97% and 17.85% respectively.

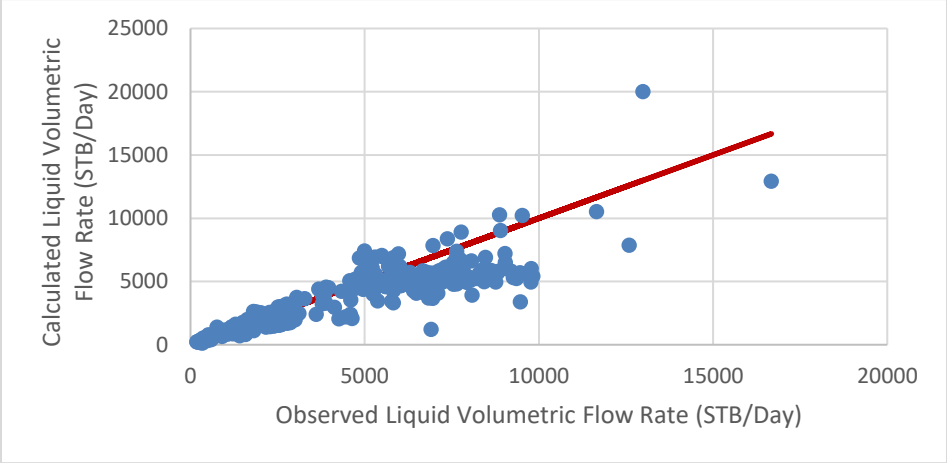

Figure 6-2: Field Data Results of Sachdeva et al. Model (1986) (Cd=0.83)

6.3.2. Sachdeva et al. Model with k/n Correction

To compare the performances with Sachdeva et al. original model, the discharge coefficient value used here is optimized by using least square method first. Then the value is manually updated until both average absolute error and standard deviation are in good ranges. The optimized Cd value was found to be approximately 0.90 for both data set.

6.3.2.1. Applied to Lab Data Set

Figure 6-3 shows figures of model performances based on 629 lab data for Sachdeva et al. Model with k/n correction. Sachdeva model with correction showed an average error of -8.90%, an average absolute error of 13.27% and standard deviation of 13.48%. For critical flow, the three evaluation criteria are -13.44%, 15.61% and 11.20% respectively. For subcritical flow, the three evaluation criteria are -3.10%, 10.27% and 13.92% respectively.

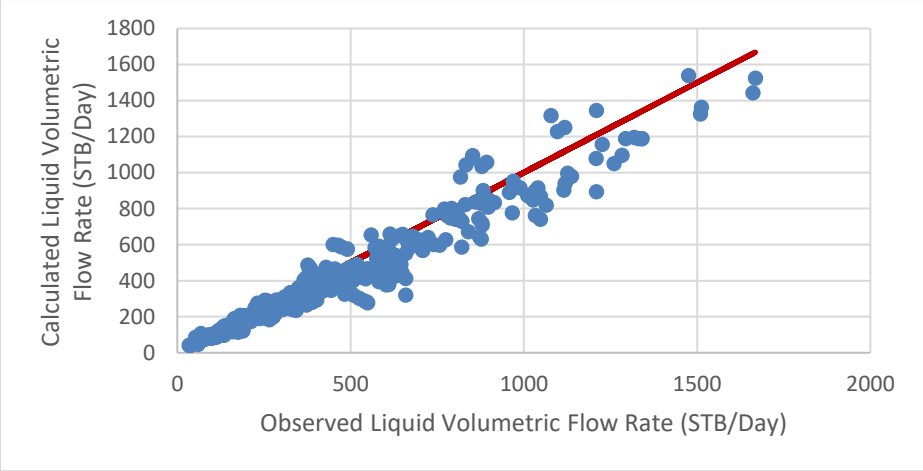

Figure 6-3: Lab Data Results of Sachdeva et al. Model with k/n Correction (Cd=0.90)

6.3.2.2. Applied to Field Data Set

Figure 6-4 shows graphical representations of model performances based on 375 field data for Sachdeva et al. Model with k/n correction. Sachdeva model with correction showed three evaluation criteria of -14.39%, 22.25% and 22.20%. For critical flow, the three evaluation criteria are -14.49%, 22.05% and 21.92% respectively. For subcritical flow, the three evaluation criteria are -14.10%, 22.83% and 23.13% respectively.

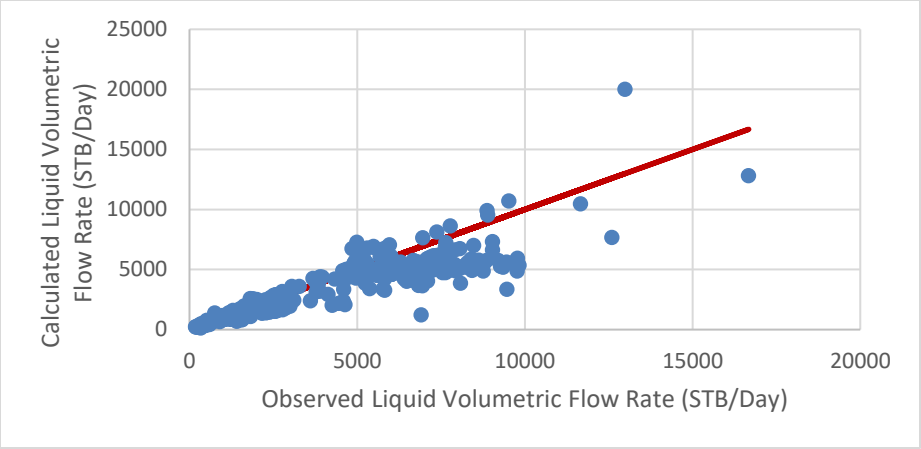

Figure 6-4: Field Data Results of Sachdeva et al. Model with k/n Correction (Cd=0.90)

6.3.3. Perkins Model

6.3.3.1. Applied to Lab Data Set

Figure 6-5 shows graphical representations of model performances based on 629 lab data for Perkins Model (1993). The optimized Cd value was found to be 0.89 for lab data. With this Cd value, Perkins model showed an average error of -9.29%, an average absolute error of 13.70% and standard deviation of 13.78%. For critical flow, the three evaluation criteria are -13.58%, 15.78% and 11.39% respectively.

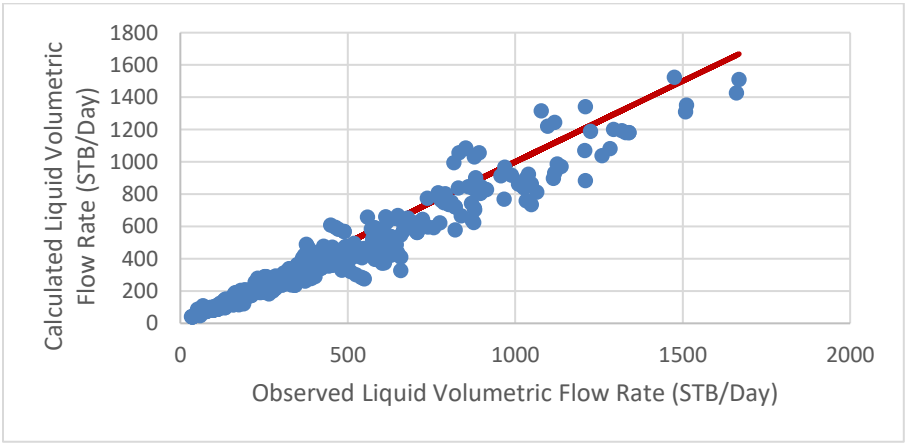

Figure 6-5: Lab Data Results of Perkins Model (1993) (Cd=0.89)

6.3.3.2. Applied to Field Data Set

Figure 6-6 shows graphical representations of model performances based on 375 field data for Perkins Model (1993). The optimized Cd value was found to be 0.905. Perkins model showed an average error of -14.43%, an average absolute error of 22.85% and standard deviation of 22.89%. For critical flow, the three evaluation criteria are -14.65%, 22.75% and 22.61% respectively. For subcritical flow, the three evaluation criteria are -10.82%, 24.50% and 27.39% respectively.

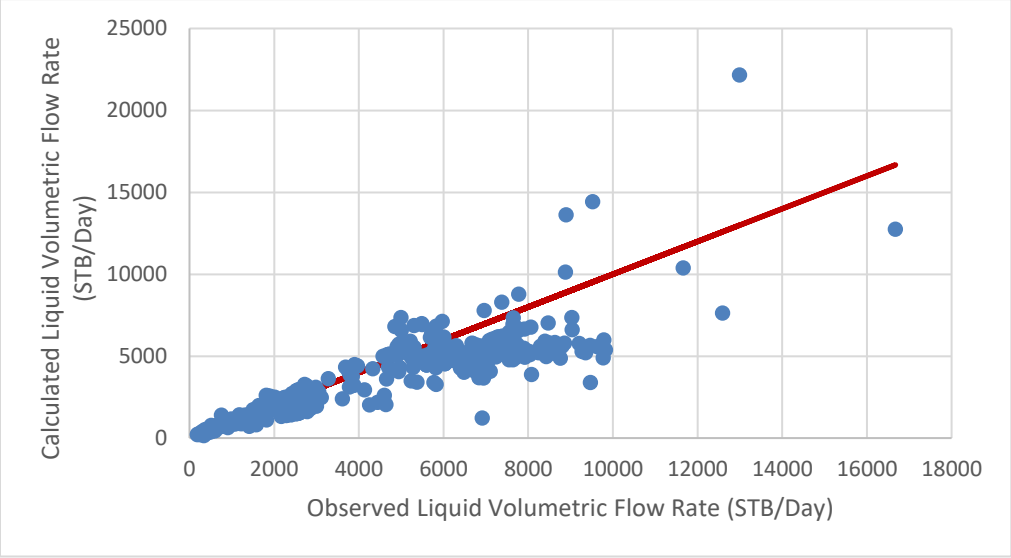

Figure 6-6: Field Data Results of Perkins Model (1993) (Cd=0.905)

6.3.4. Al-Safran and Kelkar Model

6.3.4.1. Applied to Lab Data Set

Figure 6-7 shows graphical representations of model representations based on 629 lab data for Al-Safran and Kelkar Model (2007). The optimized Cd value was found to be approximately 0.62. Al-Safran and Kelkar model showed an average error of -8.70%, an average absolute error of 16.76% and standard deviation of 17.40%. For critical flow, the

three evaluation criteria are -3.37%, 18.18% and 20.84% respectively. For subcritical flow, the three evaluation criteria are -12.53%, 15.54% and 12.96% respectively.

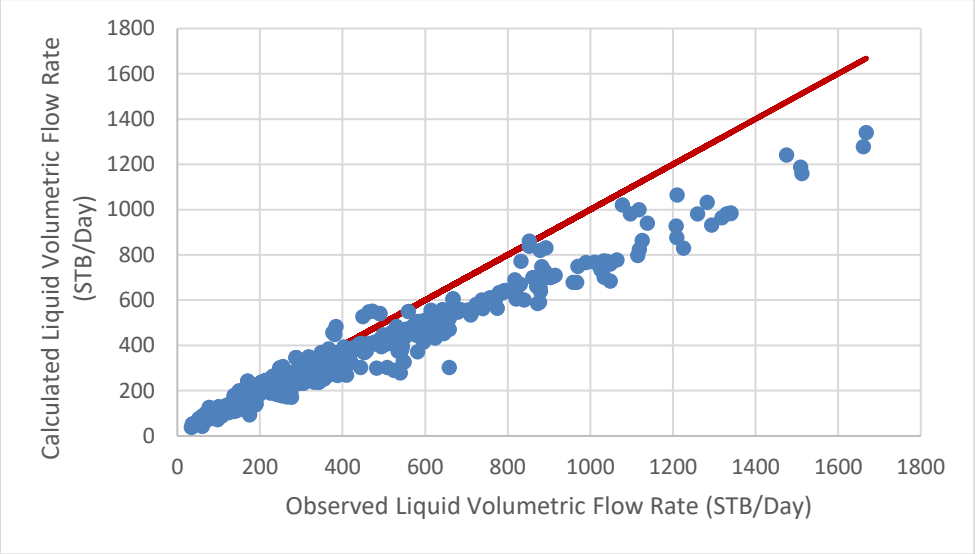

Figure 6-7: Lab Data Results of Al-Safran and Kelkar Model (2007) (Cd=0.62)

6.3.4.2. Applied to Field Data Set

Figure 6-8 shows graphical representations of model performances based on 375 field data for Al-Safran and Kelkar Model (2007). The optimized Cd value was found to be around 0.74 to 0.75, so the original 0.75 Cd value was used. Al-Safran and Kelkar model showed an average error of -14.91%, an average absolute error of 25.07% and standard deviation of 25.35%. For critical flow, the three evaluation criteria are -6.56%, 24.99% and 30.06% respectively. For subcritical flow, the three evaluation criteria are -19.24%, 25.43% and 21.65% respectively.

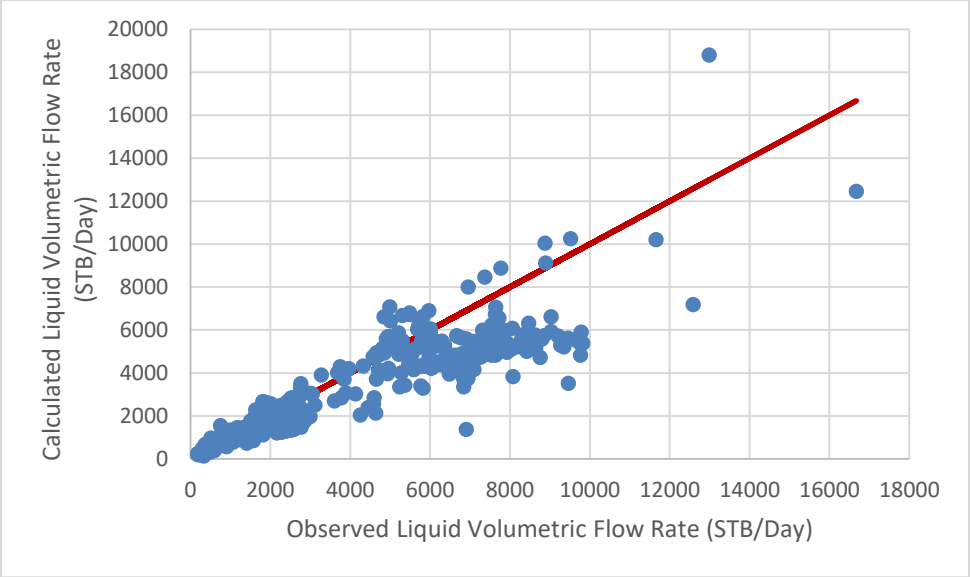

Figure 6-8: Field Data Results of Al-Safran and Kelkar Model (2007) (Cd=0.75)

6.3.5. Sachdeva et al. Model with Slip and k/n Correction

7 different slip correlations discussed in CHAPTER 2.4 were added into Sachdeva et al. model to determine if slippage effect indeed has a significant impact on performances and if so which slip correlation shows the best performance. The homogeneous (no slip) and constant slip correlations were not studied. For lab data set, the best slip correlation was found to be the constants proposed by Simpson et al. For field data set, there are three slip correlations showing similar performances. Based on the consideration of consistency, constants proposed by Simpson et al. are ranked in the first place. Because of the size limit, graphical representation is not shown for each correlation, the statistical results for different correlation are displayed in Figure 6-9 for lab data and Figure 6-10 for field data.

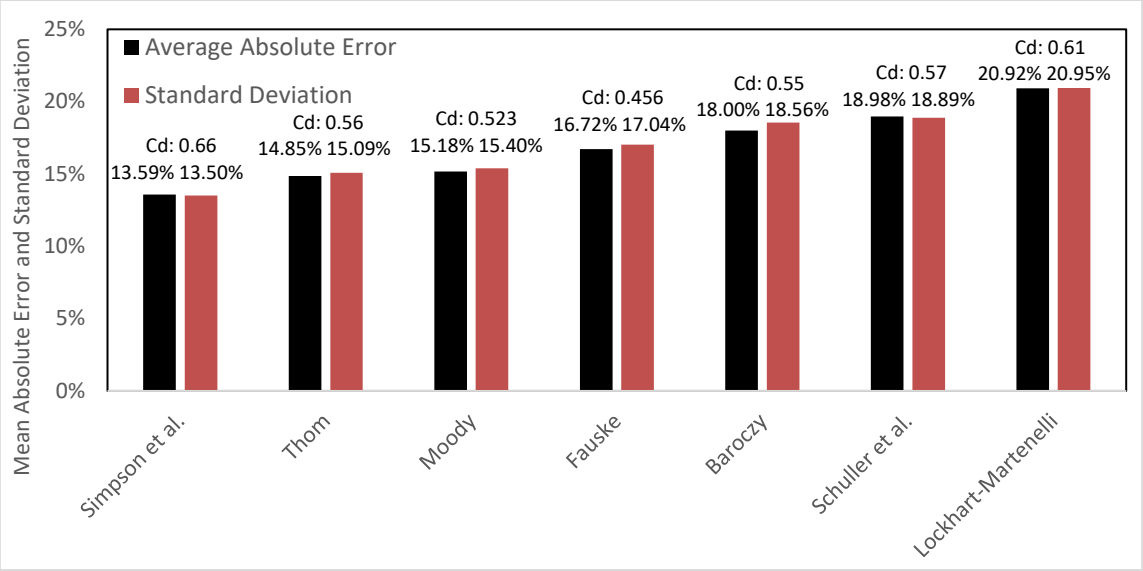

Figure 6-9: Lab Data Results for 7 Slip Equations Used on Sachdeva et al. Model

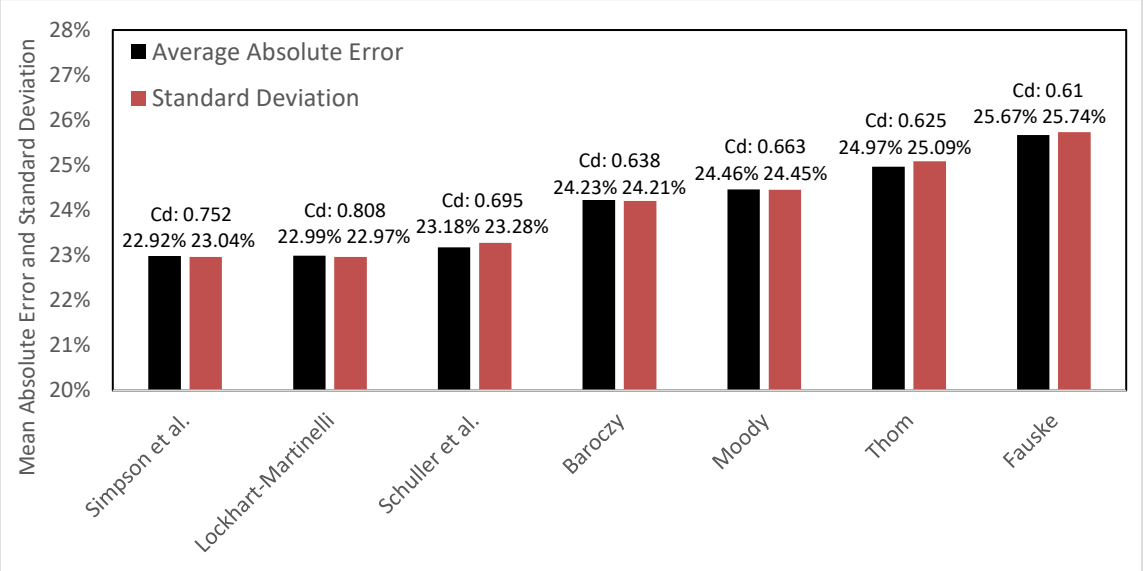

Figure 6-10: Field Data Results for 7 Slip Equations Used on Sachdeva et al. Model

Because constants proposed by Simpson et al. outperformed all other correlations for lab data evaluation and its performance is relatively good for field data evaluation, constants proposed by Simpson et al. are recommended in this study to account for

slippage effect. The following results and graphs are all generated by using slip constants proposed by Simpson et al and the Cd value used is 0.66 for lab data and 0.752 for field data.

6.3.5.1. Applied to Lab Data Set

Figure 6-11 shows graphical representations of model performances based on 629 lab data for Sachdeva model with slip (Simpson et al.). It showed an average error of -9.37%, an average absolute error of 13.59% and standard deviation of 13.50%. For critical flow, the three evaluation criteria are -12.61%, 15.43% and 12.44% respectively. For subcritical flow, the three evaluation criteria are -6.75%, 12.10% and 13.77% respectively.

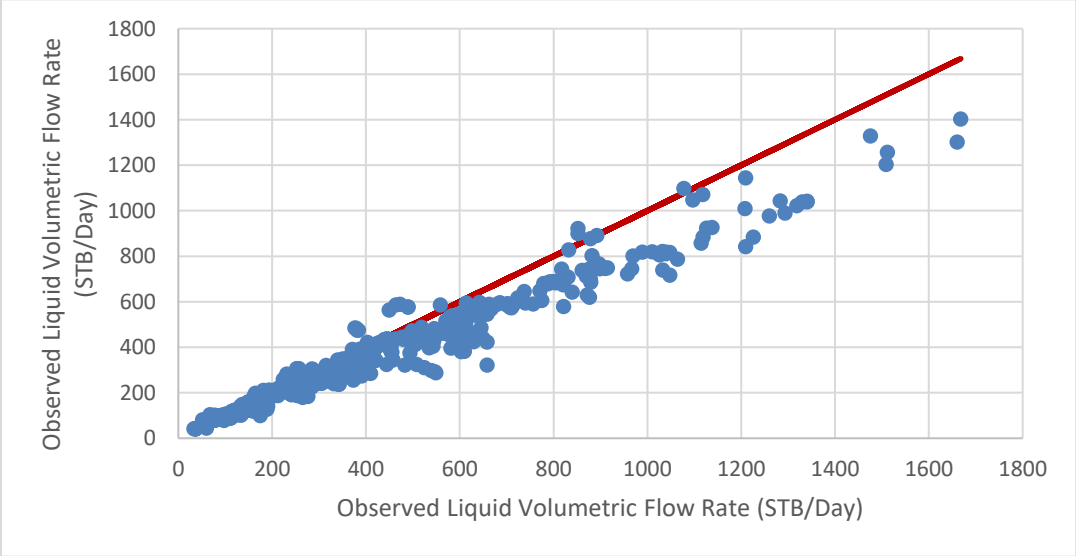

Figure 6-11: Lab Data Results of Sachdeva Model with Slip (Simpson et al.) (Cd=0.66)

6.3.5.2. Applied to Field Data Set

Figure 6-12 shows graphical representations of model performances based on 375 field data for Sachdeva model with slip (Simpson et al.). It showed an average error of -14.33%, an average absolute error of 22.92% and standard deviation of 23.04%. For

critical flow, the three evaluation criteria are -9.86%, 20.28% and 23.68% respectively. For subcritical flow, the three evaluation criteria are -16.73%, 24.34% and 22.37% respectively.

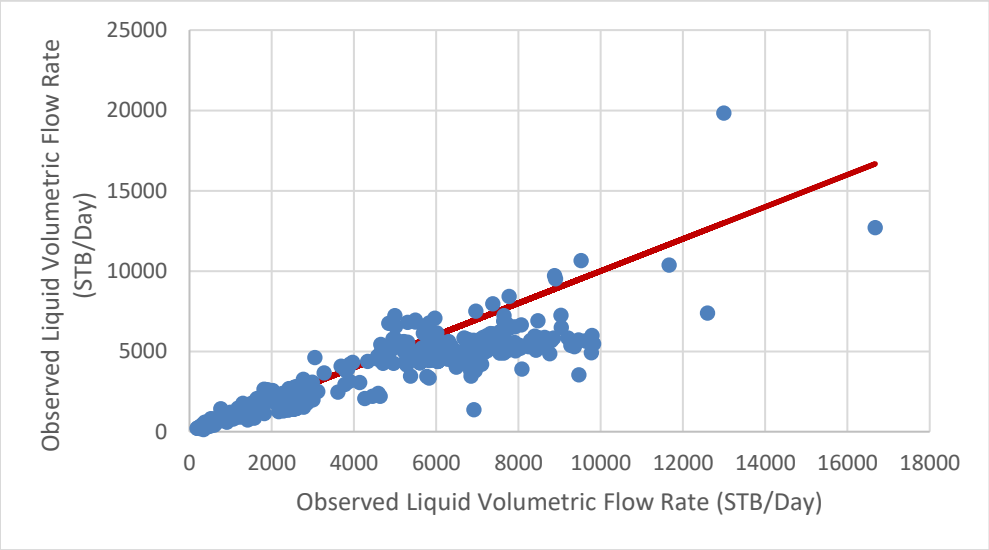

Figure 6-12: Field Data Results of Sachdeva Model with Slip (Simpson et al.) (Cd=0.752)

6.3.5.3. Slip Velocity and Slippage Effect

To further investigate the slippage effect between gas and liquid phase at choke throat condition for multiphase flow, slip velocity at choke throat condition were calculated. Concept of slip velocity was demonstrated in section 2.5. Because the slippage effect was tested for Sachdeva et al. model (1986), the choke throat pressure was calculated by using approach proposed by Sachdeva et al with k and n corrected. Based on the assumptions made during building the model, flowing temperature and mass fraction were held constant. The slip velocity was calculated for lab and field data set separately. To see the significance of slip velocity, the ratio of slip velocity to superficial gas velocity was also

calculated. For results generated based on lab data, graphical representations were shown in Figure 6-13.

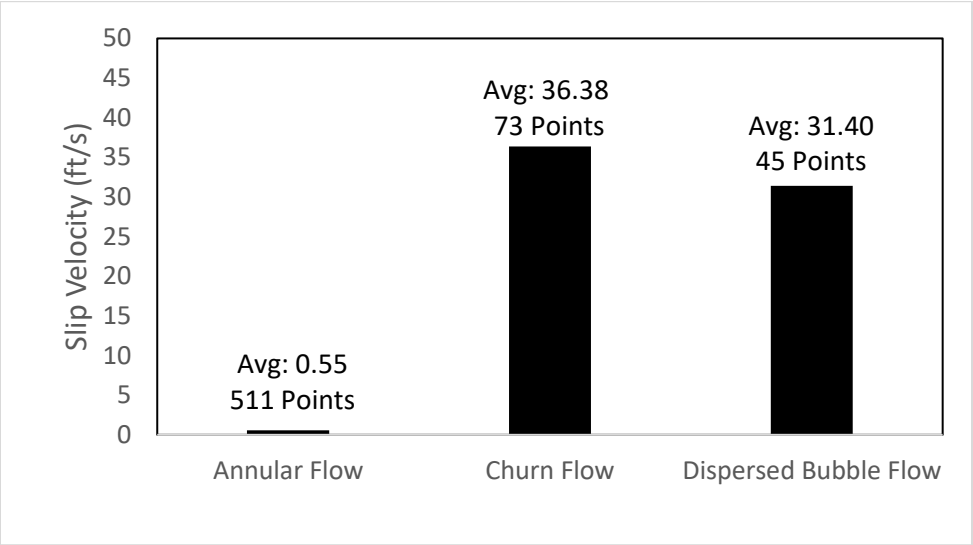

(a) Slip Velocity for Different Flow Patterns

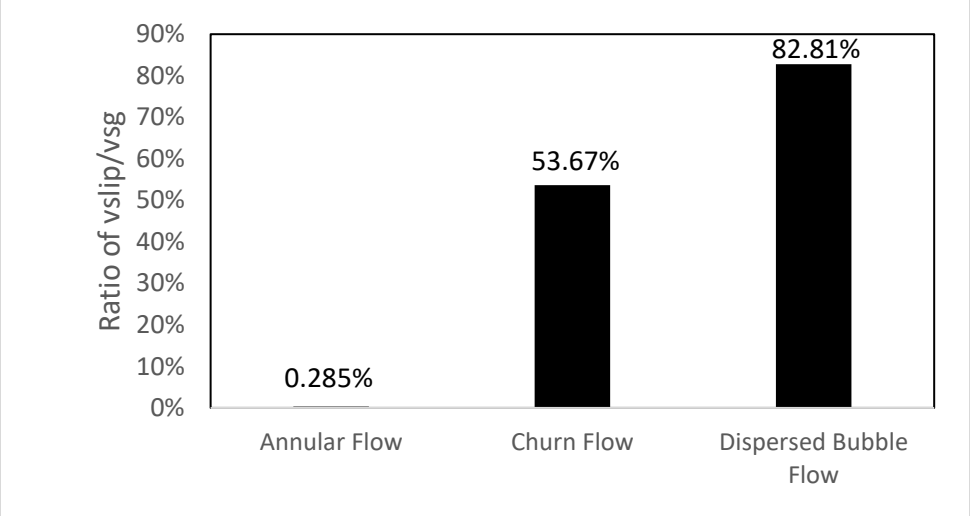

(b) Ratio of Slip Velocity/Gas Superficial Velocity for Different Flow Patterns

Figure 6-13: Slip Velocity Results for Lab Data

For the whole lab dataset, the statistical results were shown in Table 6-1:

Table 6-1: Statistical Results for Lab Slip Velocity

	Gas Superficial Velocity (ft/s)	Slip Velocity (ft/s)	Ratio of Slip/ Gas Superficial Velocity
Average Value	176.6	6.916	12.38%

For results generated based on field data, figures were shown in Figure 6-14.

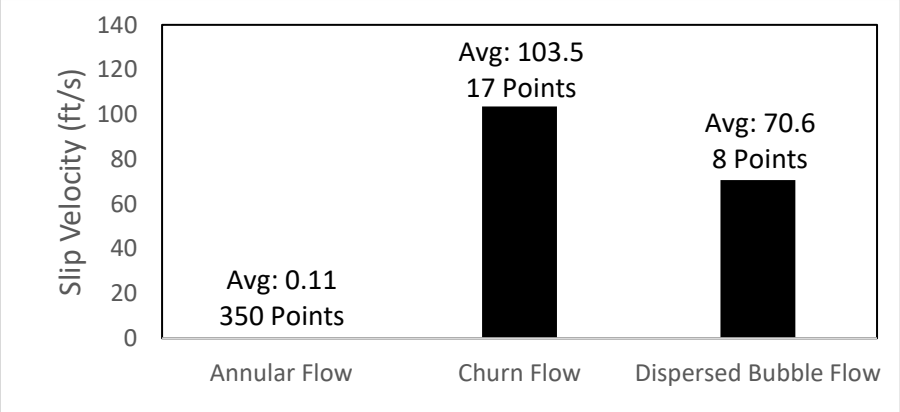

(a) Slip Velocity for Different Flow Patterns

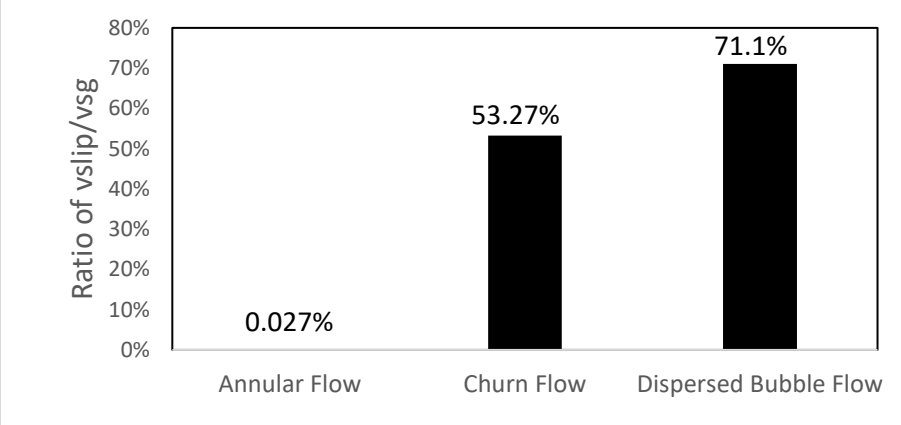

(b) Ratio of Slip Velocity/Gas Superficial Velocity for Different Flow Patterns

Figure 6-14: Slip Velocity Results for Field Data

The statistical results were also provided and shown in Table 6-2:

Table 6-2: Statistical Results for Field Slip Velocity

	Gas Superficial Velocity vsg (ft/s)	Slip Velocity (ft/s)	Ratio of Slip/ Gas Superficial Velocity
Average Value	584.1	6.335	3.96%

6.3.6. Discharge Coefficient

The discharge coefficient for Sachdeva et al. model with k/n correction was tuned based on the correction ratio required to match the calculated liquid volumetric flow rate data with the calculated data. A best-fit line was made through data points for lab and field data separately. Relationships for Cd vs. Reynolds number and Cd vs. Observed liquid volumetric flow rate were studied. Cd is normally based on Reynolds number. For simplicity, the equation can also be reduced to include only the flow rate term. Reynolds number used in this study was calculated by using Homogeneous model. Relationship was shown in Figure 6-15 for lab data. Within the figure, (a) represents figure for Cd vs. Observed liquid volumetric flow rate, (b) represents figure for Cd vs. Reynolds number.

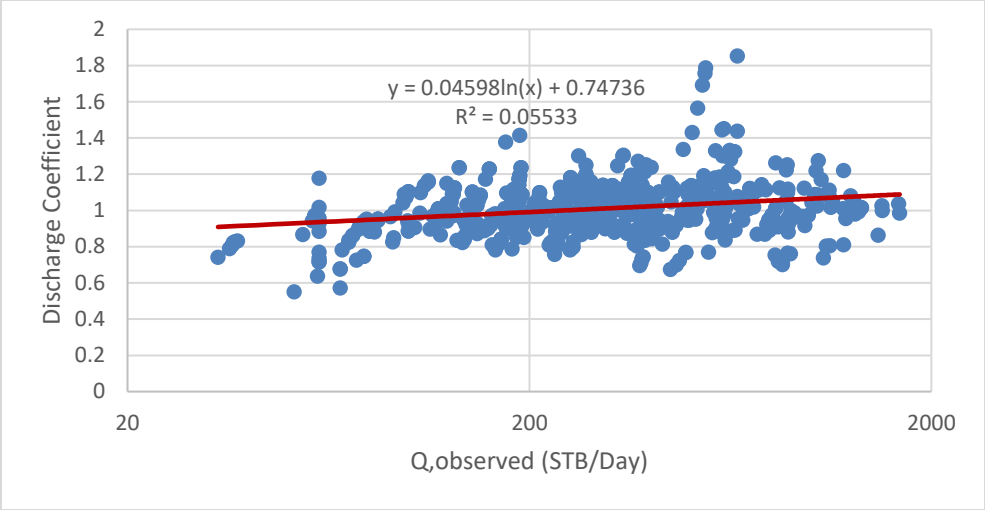

(a) Cd vs. Observed Liquid Volumetric Flow Rate

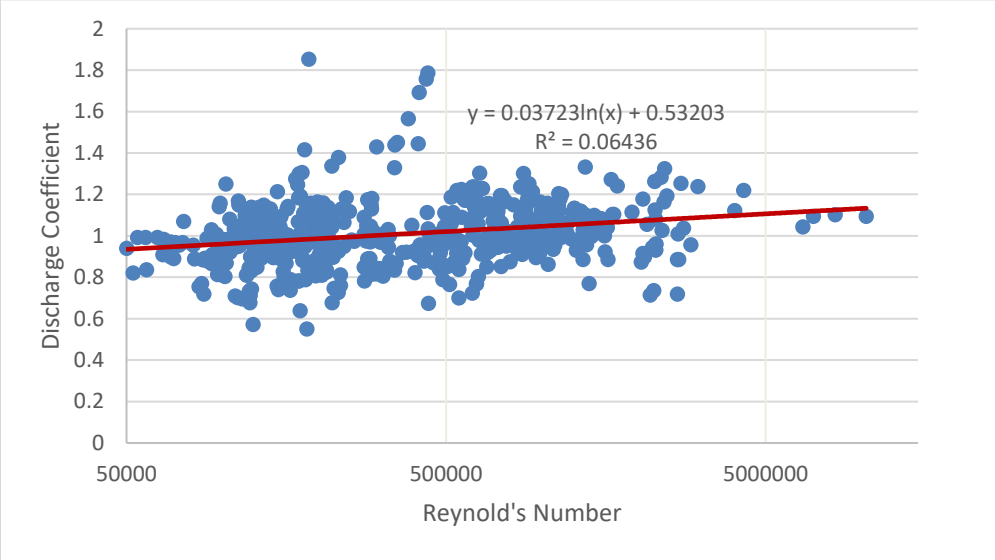

(b) Cd vs. Reynolds Number

Figure 6-15: Discharge Coefficient for Lab Data

The equations in Figure 6-15 were used to calculate discharge coefficient with the best fit line for lab data as shown in Equation (74) and (75):

$$C_d = 0.04598 \ln(Q_l) + 0.74736 \quad (74)$$

$$C_d = 0.03723 \ln(Re) + 0.53203 \quad (75)$$

Figure 6-16 was shown for field data discharge coefficient vs. observed liquid flow rate and Reynolds number.

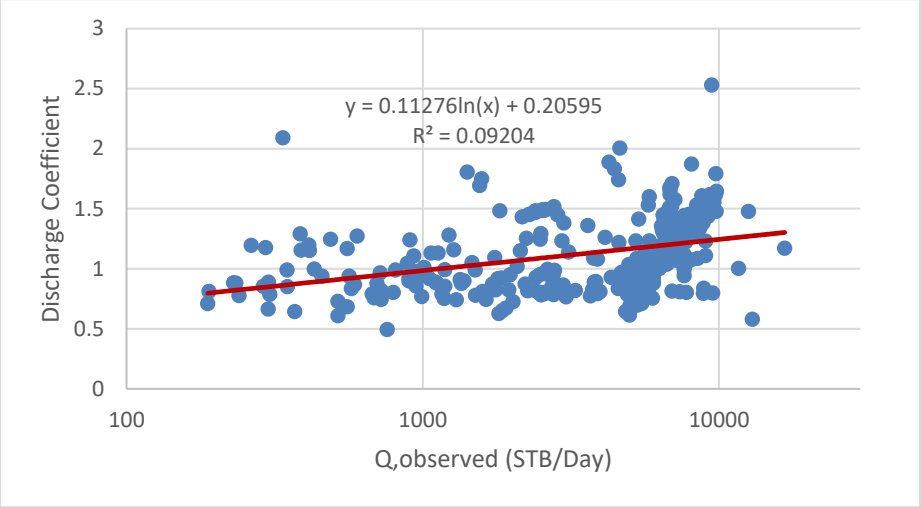

(a) Cd vs. Observed Liquid Volumetric Flow Rate

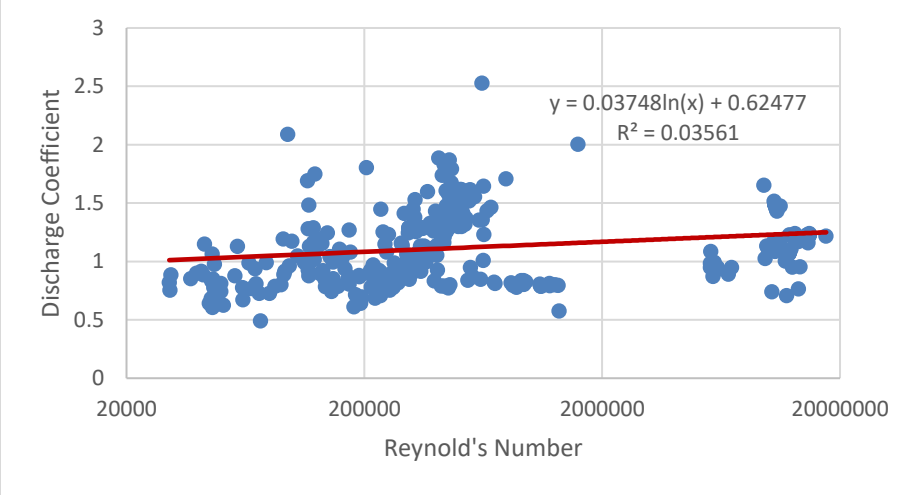

(b) Cd vs. Reynolds Number

Figure 6-16: Discharge Coefficient for Field Data

The equations in Figure 6-16 were used to calculate discharge coefficient with the best fit line for field data as shown in Equation (76) and (77):

$$C_d = 0.11276 \ln(Q_l) + 0.20595 \quad (76)$$

$$C_d = 0.03748 \ln(Re) + 0.62477 \quad (77)$$

6.4. Correlation Results

For all four correlations studied, the oil volumetric flow rate was calculated directly. If the only liquid phase is water, then these correlations can't be applied. Therefore, the single water phase flow data points are not included in evaluating correlations. There are total 249 single water phase data which are all from Sachdeva et al lab data. The missing of these 249 single water phase data points should not affect final evaluation much because these correlations were not proposed for predicting water flow rate and in the real world oil flow rate is always the most important variable the industry is interested in.

6.4.1. Fortunati Correlation

6.4.1.1. Applied to Lab Data

Fortunati (1972) proposed a discharge coefficient of 1.15 to be used for his correlation. Based on the 380 lab data used in this section, the original and optimized Cd values were tested in this study and graphical representations were shown in Figure 6-17 for results generated with optimized Cd value only. For a 1.15 discharge coefficient, the average relative error, average absolute error and standard deviation were calculated to be 29.35%, 34.01% and 35.32% respectively. For critical flow, the three evaluation criteria are –27.32%, 27.32% and 13.54% respectively. For subcritical flow, the three evaluation criteria are 30.41%, 34.13% and 34.73% respectively. For a 0.81 discharge coefficient,

the three evaluation criteria were calculated to be -8.89%, 18.81% and 24.88% respectively. For critical flow, the three evaluation criteria are -48.81%, 48.81% and 9.53% respectively. For subcritical flow, the three evaluation criteria are -8.14%, 18.25% and 24.46% respectively.

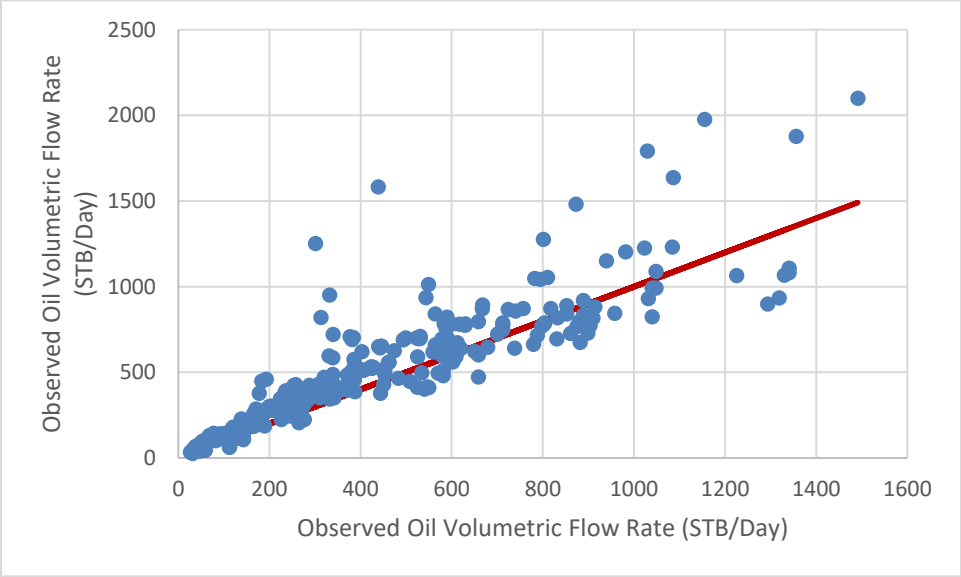

Figure 6-17: Lab Data Results of Fortunati Correlation (1972) (Cd=0.81)

6.4.1.2. Applied to Field Data

Based on the evaluation of 375 field data points, the 1.15 Cd value was tested in this study. The average relative error, average absolute error and standard deviation were calculated to be -17.47%, 32.87% and 35.36% respectively.

The optimized Cd value was calculated to be 1.08. The corresponding average relative error, average absolute error and standard deviation were calculated to be -22.50%, 33.47% and 33.20% respectively. Even though the average absolute error was not improved but decreased 0.6%, the standard deviation results was improved almost 2%. By

sacrificing 0.6% absolute error, it is worthy to improve standard deviation 2%. For critical flow, the three evaluation criteria are -63.79%, 63.79% and 13.24% respectively. For subcritical flow, the three evaluation criteria are -13.83%, 27.12% and 29.40% respectively. The results were shown in Figure 6-18.

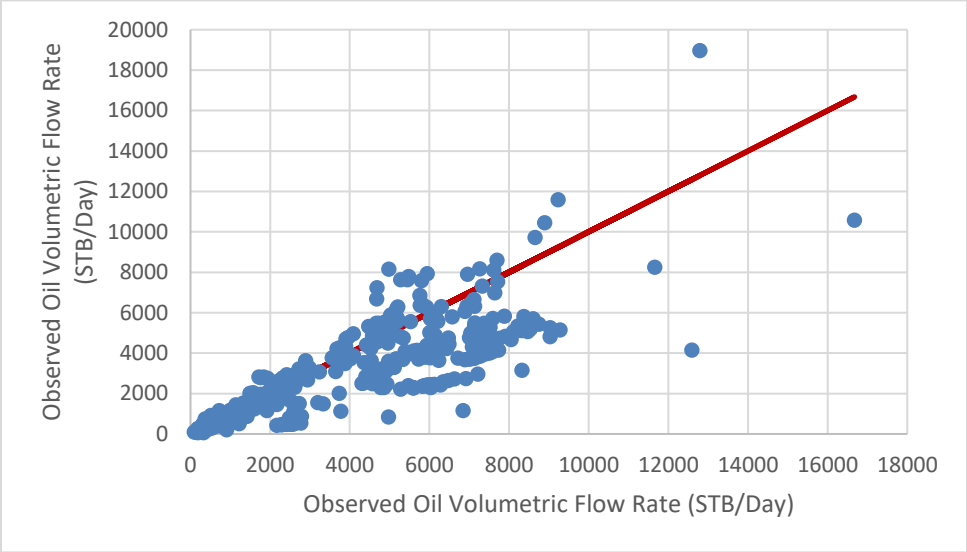

Figure 6-18: Field Data Results of Fortunati Correlation (1972) (Cd=1.08)

6.4.2. Ashford and Pierce Correlation

Ashford and Pierce (1975) proposed three different discharge coefficients to be used for three different choke openings evaluated in their study. Al-Attar then determined discharge coefficients of three additional choke diameters for Ashford and Pierce subcritical correlation using the operational conditions found in his study.

Table 6-3 shows the observed Cd values proposed by Ashford and Pierce (1975) and Al-Attar (2010) and calculated Cd values by using equations generated from observed values. The equations for choke sizes ranging from 14 to 20/64th inch and 64 to 144/64th inch are shown in Equation (78) and Equation (79):

$$Cd_{Ash} = 0.004533(d_c)^2 - 0.1833d_c + 2.82867 \quad (78)$$

$$Cd_{Al-Attar} = -1.487\times10^{-5}(d_c)^2 - 1.1958\times10^{-3}d_c + 0.94824 \quad (79)$$

Figure 6-19 shows a graphical representation of discharge coefficients against choke size and how these points are fitted into equations above. The equations generated can be used to calculate corresponding Cd values accurately with negligible relative error. The Cd values for choke diameters between 20/64th inch and 64/64th inch can be calculated by using interpolation method.

Table 6-3: Observed and Calculated Cd Values for Ashford and Pierce Correlation

Choke Size (/64th inch)	Observed Cd Value	Calculated Cd Value	Relative Error
14	1.151	1.150935	0.005647%
16	1.0564	1.056315	0.008046%
20	0.976	0.975867	0.013627%
64	0.8108	0.810799	0.000079%
96	0.6964	0.696398	0.000230%
144	0.4677	0.467696	0.000821%

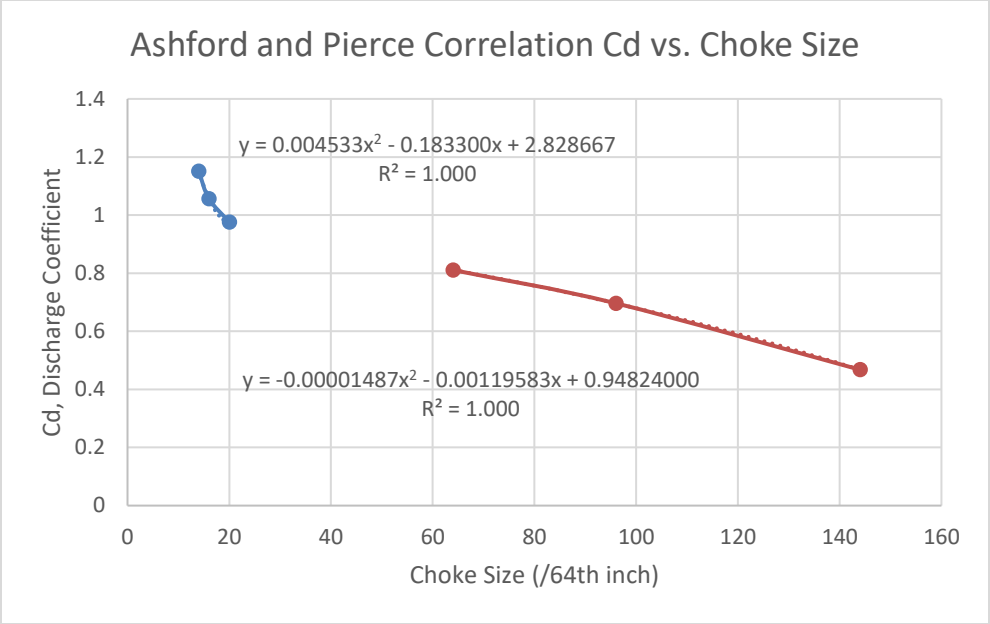

Figure 6-19: Discharge Coefficient Values for Ashford and Pierce Correlation (1975)

6.4.2.1. Applied to Lab Data

With the discharge coefficient values calculated by Equation (78) and (79). The average relative error, average absolute error and standard deviation were calculated to be 16.00%, 30.16% and 38.04% respectively. For critical flow, the three evaluation criteria are 7.17%, 12.14% and 15.06% respectively. For subcritical flow, the three evaluation criteria are 18.71%, 35.67% and 42.32% respectively. However, by using the least square method, the discharge coefficient can be optimized. Instead of a relationship with choke diameter, the updated Cd value was found to be fixed at 0.72. The average relative error, average absolute error and standard deviation were calculated to be -11.18%, 24.28% and 31.48% respectively. For critical flow, the three evaluation criteria are -22.20%, 22.27% and 9.48% respectively. For subcritical flow, the three evaluation criteria are -7.82%,

24.89% and 34.91% respectively. The graphical representations for results generated by using optimized Cd value were shown in Figure 6-20.

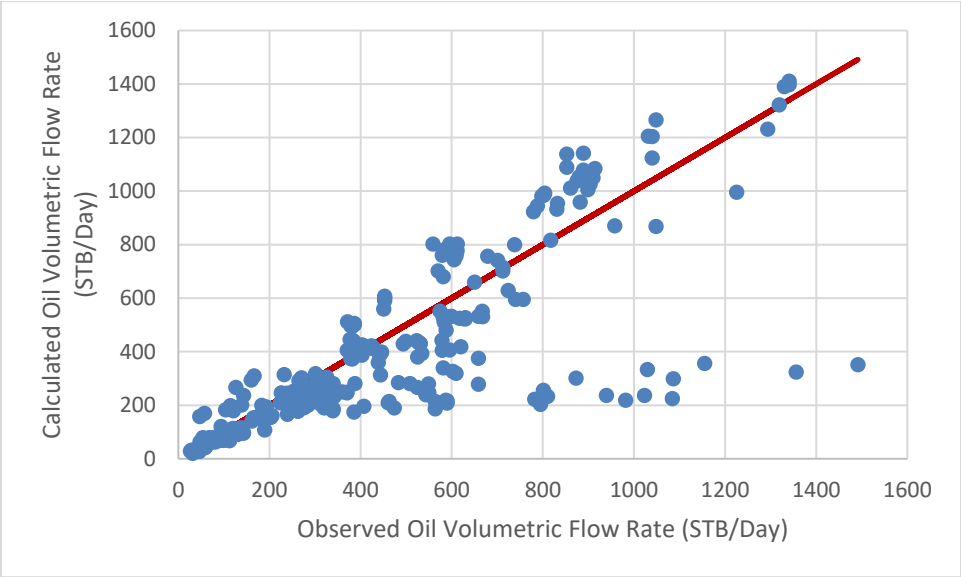

Figure 6-20: Lab Data Results of Ashford and Pierce Correlation (1975) (Cd=0.72)

6.4.2.2. Applied to Field Data

With the discharge coefficient values calculated by Equation **(78)** and **(79)**. The average relative error, average absolute error and standard deviation were calculated to be 11.20%, 40.65% and 59.95% respectively. For critical flow, the three evaluation criteria are -44.33%, 54.33% and 35.73% respectively. For subcritical flow, the three evaluation criteria are 23.06%, 37.73% and 57.39% respectively. However, by using the least square method, the discharge coefficient can be optimized. Instead of a relationship with choke diameter, the updated Cd value was found to be fixed at 0.53. The average relative error, average absolute error and standard deviation were calculated to be -23.08%, 39.73% and 39.55% respectively. For critical flow, the three evaluation criteria are -53.78%, 54.62%

and 18.30% respectively. For subcritical flow, the three evaluation criteria are -16.52%, 36.55% and 39.82% respectively. The graphical representations for results generated by using optimized Cd value were shown in Figure 6-21.

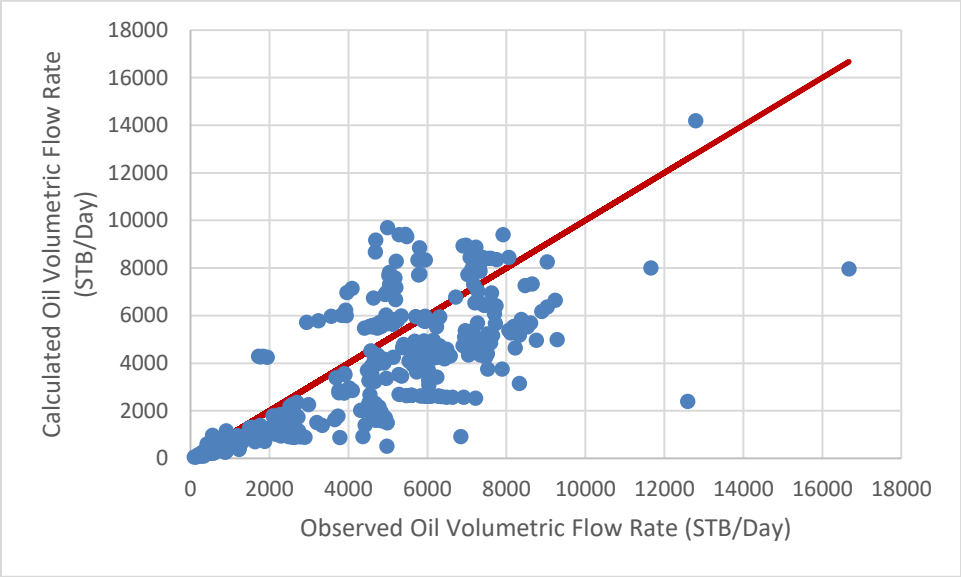

Figure 6-21: Field Data Results of Ashford and Pierce Correlation (1975) (Cd=0.53)

6.4.3. Al-Attar Correlation

6.4.3.1. Applied to Lab Data

Figure 6-22 shows graphical representations of correlation performances based on lab data for Al-Attar Correlation (2010). It showed an average error of -2.80%, an average absolute error of 73.76% and standard deviation of 104.12%. Because this correlation does not have a discharge coefficient value originally, so discharge coefficient is not added.

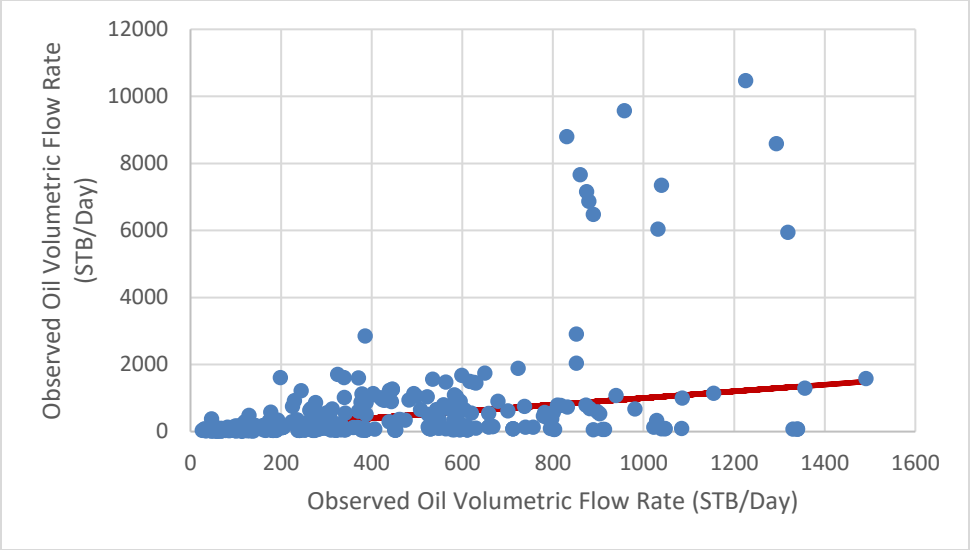

Figure 6-22: Lab Data Results of Al-Attar Correlation (2010)

6.4.3.2. Applied to Field Data

Figure 6-23 shows graphical representations of correlation performances based on field data for Al-Attar Correlation (2010). It showed an average error of -10.55%, an average absolute error of 74.55% and standard deviation of 131.15%.

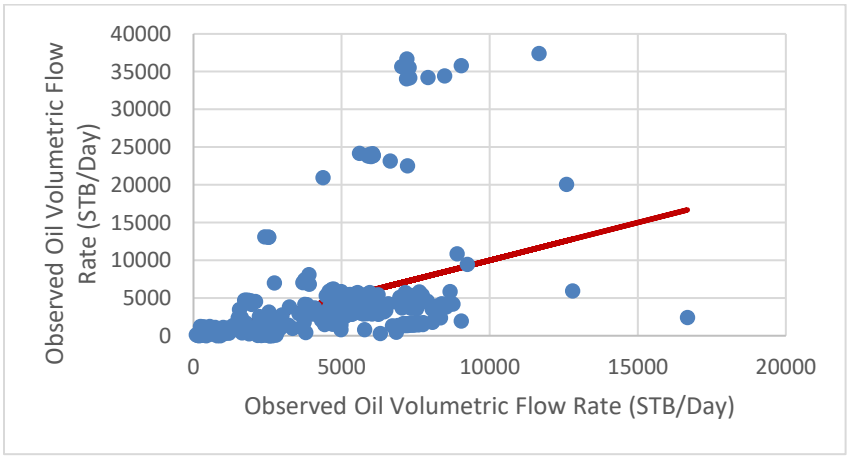

Figure 6-23: Field Data Results of Al-Attar Correlation (2010)

6.4.4. B-K Correlation

6.4.4.1. Applied to Lab Data

Figure 6-24 shows graphical representations of correlation performances based on lab data for B-K Correlation (2012). It showed an average error of -124.93%, an average absolute error of 125.57% and standard deviation of 165.82%. Because this correlation does not have a discharge coefficient value originally, so discharge coefficient is not added.

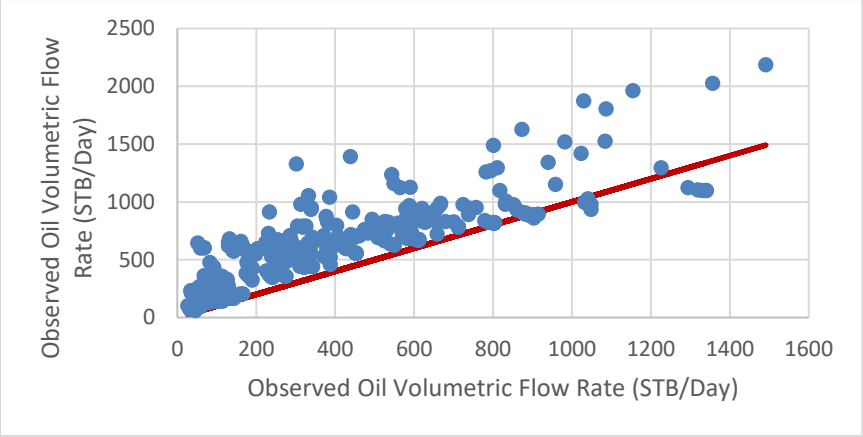

Figure 6-24: Lab Data Results of B-K Correlation (2012)

6.4.4.2. Applied to Field Data

Figure 6-25 shows graphical representations of correlation performances based on field data for B-K Correlation (2012). It showed an average error of -29.99%, an average absolute error of 50.27% and standard deviation of 102.67%.

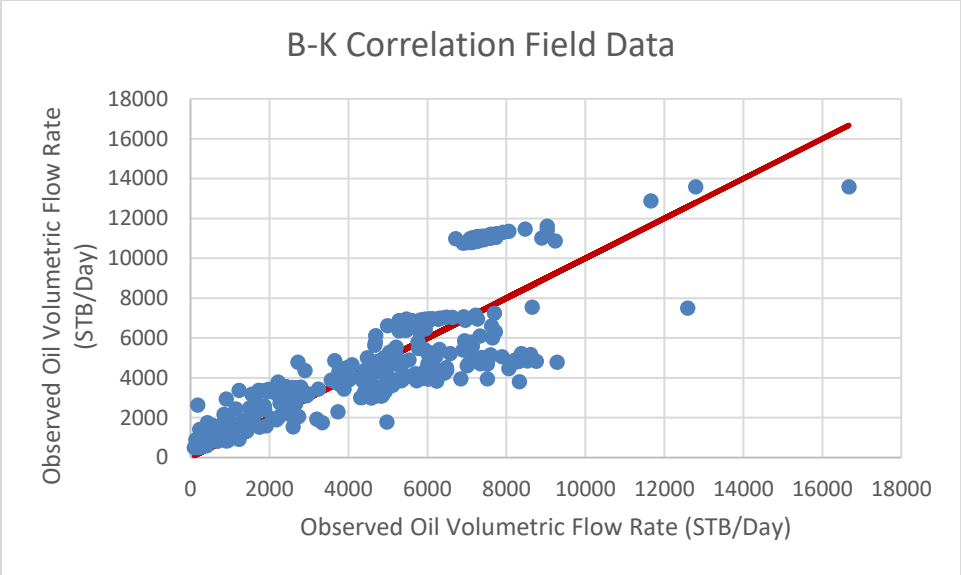

Figure 6-25: Field Data Results of B-K Correlation (2012)

7 DISCUSSIONS

7.1. Evaluated Models Discussion

7.1.1. Sachdeva et al. Model

For lab data, the model both underestimate and overestimate liquid flow rate. There is no obvious difference between critical and subcritical flow error analysis.

For field data, the model both underestimate and overestimate liquid flow rate. The model predicted subcritical flow better than critical flow.

7.1.2. Sachdeva et al. Model with k/n Correction

For lab data, with this correction, the performance was not as good as the model without correction. Average absolute error and standard deviation were decreased by 1% and 0.61% respectively. There is no obvious difference between critical and subcritical flow error analysis.

For field data, with this correction, average absolute error was decreased by 0.28% and standard deviation was improved by 0.91%. There is no obvious difference between critical and subcritical flow error analysis.

As can be seen, the accuracy difference between model with correction and without correction was negligible and the correction failed to improve prediction accuracy and stability. Though significant improvement on accuracy was not observed, this correction was recommended from theoretical point of view.

7.1.3. Perkins Model

For lab data, the model performance was not as good as Sachdeva et al model with correction. Average absolute error and standard deviation were decreased by 1.18% and

0.27% respectively compared to Sachdeva et al. model with k/n correction. the model both underestimate and overestimate liquid flow rate. There is no obvious difference between critical and subcritical flow error analysis.

For field data, the performance between Perkins model and Sachdeva et al model with correction was small. Average absolute error and standard deviation were decreased by 1.08% and 0.08% respectively compared to Sachdeva et al. model with k/n correction. The model both underestimate and overestimate liquid flow rate. The model predicted subcritical flow better than critical flow.

7.1.4. Kelkar Model

For lab data, the model both underestimate and overestimate liquid flow rate. The model predicted subcritical flow better than critical flow. For subcritical flow, the average absolute error and standard deviation were 2.64% and 7.88% better than critical flow respectively. The model performance was not as good as Sachdeva et al model with correction. Average absolute error and standard deviation were decreased by 4.44% and 3.62% respectively.

For field data, the model both underestimate and overestimate liquid flow rate. The model predicted subcritical flow better than critical flow. For subcritical flow, though the average absolute error was 0.44% worse but standard deviation was 8.41% better than critical flow. The model performance was not as good as Sachdeva et al model with correction. Average absolute error and standard deviation were decreased by 3.32% and 2.66% respectively.

7.1.5. Sachdeva et al. Model with Slip (Simpson et al.)

Both Al-Safran and Kelkar (2007) and Juliana and Milan (2016) showed the slip ratio should be considered into Sachdeva et al model (1986) for better performances. Because Sachdeva et al. model (1986) shows the best prediction performance compared to Perkins model (1993) and Al-Safran and Kelkar model (2009), the slippage effect was added into Sachdeva et al. model (1986) to see if it can be further improved.

For lab data, the model both underestimate and overestimate liquid flow rate, there is no obvious difference between critical and subcritical flow error analysis. The average absolute error was improved 0.98%, the standard deviation was decreased by 0.78% compared to Sachdeva et al. model with correction.

For field data, the model both underestimate and overestimate liquid flow rate, there is no obvious difference between critical and subcritical flow error analysis. The average absolute error and standard deviation were decreased by 0.63% and 1.11% respectively compared to Sachdeva et al. model with correction.

7.1.6. Overall Discussions on Models Evaluated

To show a direct comparison on performances between Sachdeva et al. model with k/n correction and other models, Table 7-1 and Table 7-2 were created. The negative value means the evaluated model was not as good as Sachdeva et al. model with k/n correction. The positive value means the evaluated model showed a better performance than Sachdeva et al. model with k/n correction for that criteria. The graphical representatives were also generated and shown in Figure 7-1 and Figure 7-2. As can be seen, the model with best performance was Sachdeva et al. model. The slippage effect showed some positive results

for lab data but overall failed to help improve prediction accuracy and stability. Hence, slippage effect was not recommended to include in Sachdeva et al. model.

Table 7-1: Lab Data Error Compared to Sachdeva et al. Model with k/n Correction

Compared to Sachdeva et al. model with k/n correction	Average Error	Average Absolute Error	Standard Deviation
Sachdeva et al. model	-2.92%	1.94%	0.30%
Perkins model	-0.31%	-0.24%	-0.57%
Al-Safran and Kelkar model	-0.20%	-3.49%	-3.92%
Sachdeva et al. model with both slip and k/n correction	-6.67%	1.93%	-1.09%

Table 7-2: Field Data Error Compared to Sachdeva et al. Model with k/n Correction

Compared to Sachdeva et al. model with k/n correction	Average Error	Average Absolute Error	Standard Deviation
Sachdeva et al. model	-4.60%	0.78%	-1.40%
Perkins model	0.99%	-0.58%	-0.57%
Al-Safran and Kelkar model	0.52%	-2.82%	-3.15%
Sachdeva et al. model with both slip and k/n correction	-2.90%	-0.13%	-1.61%

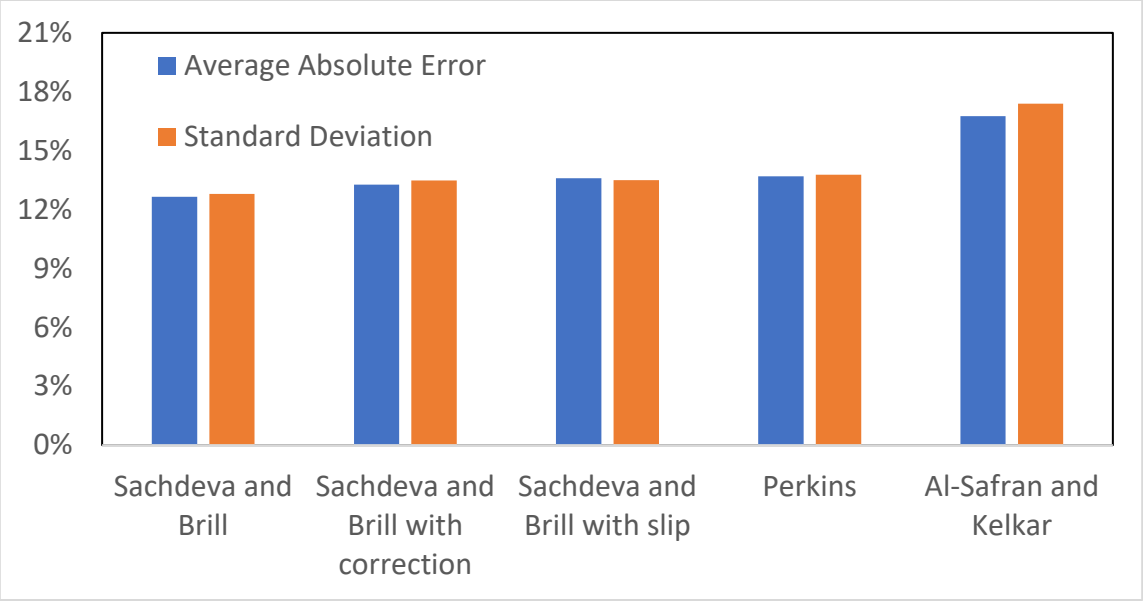

Figure 7-1: Lab Performance Comparison for All Models Studied

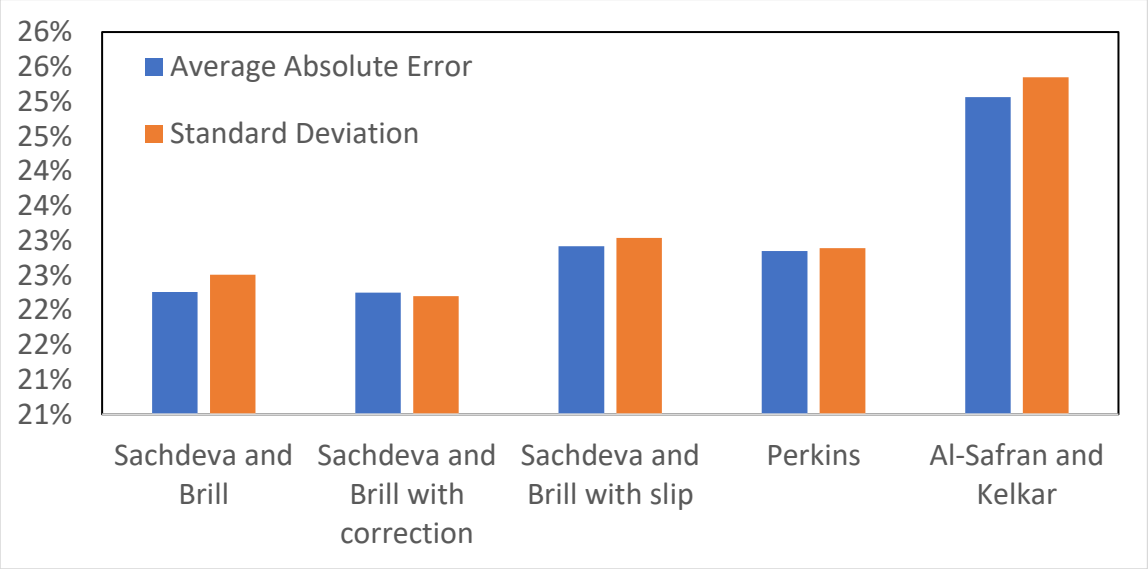

Figure 7-2: Lab Performance Comparison for All Models Studied

The following common observations were found and applied to all models evaluated. Therefore, these observations may occur due to the natural properties of data set.

Overall, for lab data, when the gas mass fraction was below 0.05, model tends to underestimate liquid flow rate. There is not enough data point available for high gas mass fraction. There is no obvious relationship observed between error and actual pressure ratio.

For field data, the error mainly occurs when the gas mass fraction was between 0 and 0.01. When the gas mass fraction was bigger than 0.3, the model tends to underestimate liquid flow rate. When the range of actual pressure ratio was between 0.5 and 0.6, prediction error tends to increase but the reason could be that more data points are within this range. the overestimated error mainly stays in actual pressure ratio ranging from 0.4 to 0.6.

There is no obvious relationship observed between prediction error and choke diameter for both lab and field data.

7.1.7. Discussion on Slippage Effect

To further investigate and explain phenomenon observed for slippage effect. The slip velocity discussed in CHAPTER 2.5 was calculated and results were shown in CHAPTER 6.3.5.3. For field data, both the average value of slip velocity and the ratio of slip velocity/ gas superficial velocity were small enough for making a conclusion that slippage effect was not important for field multiphase flow modeling through chokes. For lab data, both average value of slip velocity and ratio of slip velocity/ gas superficial velocity were higher than those of field data set, this was because the experimental conditions prepared for lab data are usually in ideal conditions. In addition, because experimental conditions are prepared manually the inputs acquired are very accurate and stable. However, for field conditions, most of the time it is extremely hard to accurately measure the inputs such as

pressure, temperature, GOR and so on. The uncertainty of field data absorbed parts of slippage effect. This explained why Al-Safran and Kelkar (2009) and Juliana and Milan (2016) observed important improvement by including slippage effect for lab data. From results provided by Al-Safran an Kelkar (2009), the performance of model with slippage effect for field data was not as good as results for lab data and the model with slip was outperformed by Perkins model.

On the other hand, by using the homogeneous model to calculate flow patterns, the results showed that most flow patterns are annular or mist flow. Kabir and Hasan (2004) proved that homogeneous model was as good as other sophisticated models when evaluating for gas/condensate wells. In addition, when annular/mist flow occurs, gas phase tends to carry liquid phase rising through pipe and choke. The difference between gas phase and liquid phase were found to be much smaller than other flow patterns. Consequently, the slippage effect for annular/mist flow is considered as negligible.

For lab data results shown in CHAPTER 6.3.5.3, there are 511 annular flow out of 629 in total. The annular flow took approximately 81.2% of total data points. The ratio of slip velocity/ gas superficial velocity for annular flow was 0.284%. For field data, there are 350 annular flow out of 375 in total. The annular flow took approximately 93.3% of total data points. The ratio of slip velocity/ gas superficial velocity for annular flow was 0.027%. Again, these results explained why slippage effect was not important for field data at all and slippage effect for lab data was more obvious that that for field data. The results also supported the conclusion that slippage effect was negligible for annular/mist flow.

7.2. Evaluated Correlations Discussions

7.2.1. Fortunati Correlation

For lab data, the correlation both underestimate and overestimate oil flow rate. The performance of critical flow was better than subcritical flow. All critical flow points were underestimated. For subcritical flow, correlation both underestimate and overestimate. For critical flow, the average absolute error and standard deviation were 6.81% and 21.19% respectively better than subcritical flow. The error tended to increase with gas mass fraction but needed more high gas mass fraction lab data. This behavior was also observed from all models evaluated, so this can be considered as the consequence of natural data.

For field data, the model both underestimate and overestimate liquid flow rate. The model predicted subcritical flow better than critical flow on absolute error but not standard deviation. All critical flow points were underestimated. For subcritical flow, this correlation both underestimate and overestimate. The pattern of error vs. gas mass fraction was similar compared to figures generated for models studied, so this can be considered as the consequence of natural data.

7.2.2. Ashford and Pierce Correlation

For lab data, the correlation both underestimate and overestimate oil flow rate. The performance of critical flow was better than subcritical flow. Almost all critical flow points were underestimated. For subcritical flow, correlation both underestimate and overestimate. For critical flow, the average absolute error and standard deviation were 2.62% and 25.43% respectively better than subcritical flow. The error tended to decrease

with gas mass fraction but needed more high gas mass fraction lab data. This behavior was opposite to what was observed for models.

For field data, the model both underestimate and overestimate liquid flow rate. The model predicted subcritical flow better than critical flow on absolute error but not standard deviation. Almost all critical flow points were underestimated. For subcritical flow, this correlation both underestimate and overestimate. The pattern of error vs. gas mass fraction was similar compared to figures generated for models studied, so this can be considered as the consequence of natural data.

7.2.3. Al-Attar Correlation

For lab data, the correlation both underestimate and overestimate oil flow rate. Because this correlation can't distinguish flow boundary, results on different flow type were not provided. The error tended to decrease with gas mass fraction but needed more high gas mass fraction lab data. Error also tended to increase with actual pressure ratio and choke diameter. These behaviors were not observed for models and Fortunati correlation.

For field data, the model both underestimate and overestimate liquid flow rate. The patterns of error vs. gas mass fraction, actual pressure ratio and choke diameter were not similar as models evaluated and Fortunati correlation.

The reason why relatively large error was generated and big difference between this correlation and evaluated models on graphical representations was because the empirical coefficients and input information for Al-Attar correlation were generated for a particular

field, which were not supposed to be applied universally. However, the approaches proposed by Al-Attar may be recommended.

7.2.4. B-K Correlation

For lab data, the correlation both underestimate and overestimate oil flow rate but mainly underestimate. Because this correlation can't distinguish flow boundary, results on different flow type were not provided. The error tended to increase with gas mass fraction but needed more high gas mass fraction lab data. Error also tended to increase with actual pressure ratio. These behaviors were not observed for models and Fortunati correlation.

For field data, the model both underestimate and overestimate liquid flow rate. The patterns of error vs. gas mass fraction, actual pressure ratio and choke diameter were not similar as models evaluated and Fortunati correlation. Error tended to decrease with choke diameter.

The reason why relatively large error was generated and big difference between this correlation and evaluated models on graphical representations was because the empirical coefficients for B-K correlation were generated for a particular field, which were not supposed to be applied universally. In addition, by only including 5 parameters when calculating oil flow rate, the process was supposed to be more complicated. If any input of these 5 parameters was not measured accurately, then the correlation has a high risk to fail.

7.2.5. Overall Discussion for Correlations

As shown in Figure 7-3 and Figure 7-4, it is apparently that Fortunati correlation and Ashford and Pierce Correlation outperformed the other two based on either lab or field

data. For Fortunati correlation and Ashford and Pierce correlation, both correlations can distinguish flow boundary. However, performance of Fortunati correlation on absolute error and standard deviation was better than Ashford and Pierce correlation, so Fortunati correlation was recommended in this study.

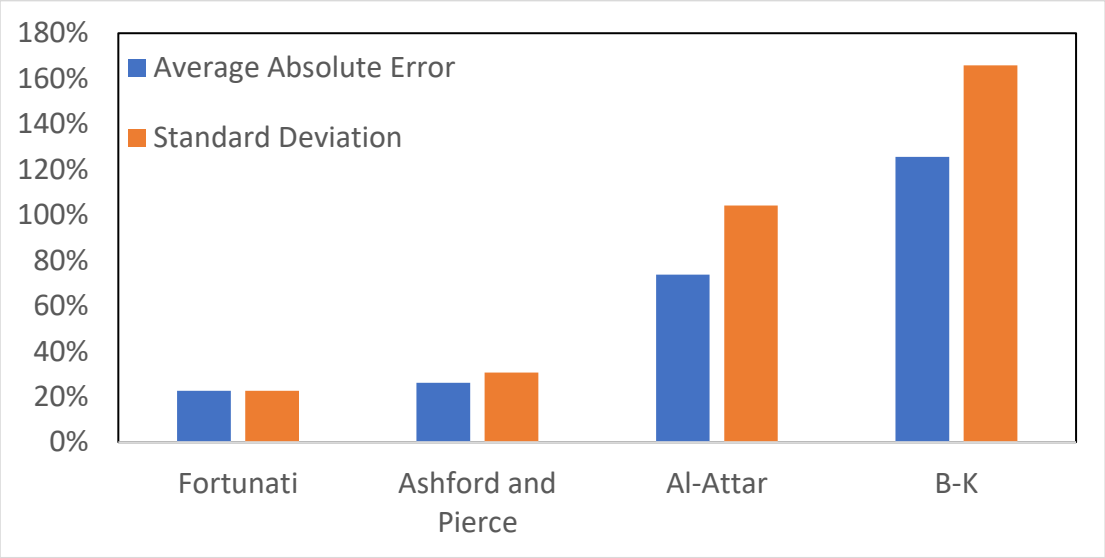

Figure 7-3: Lab Performance Comparison for Correlations Studied

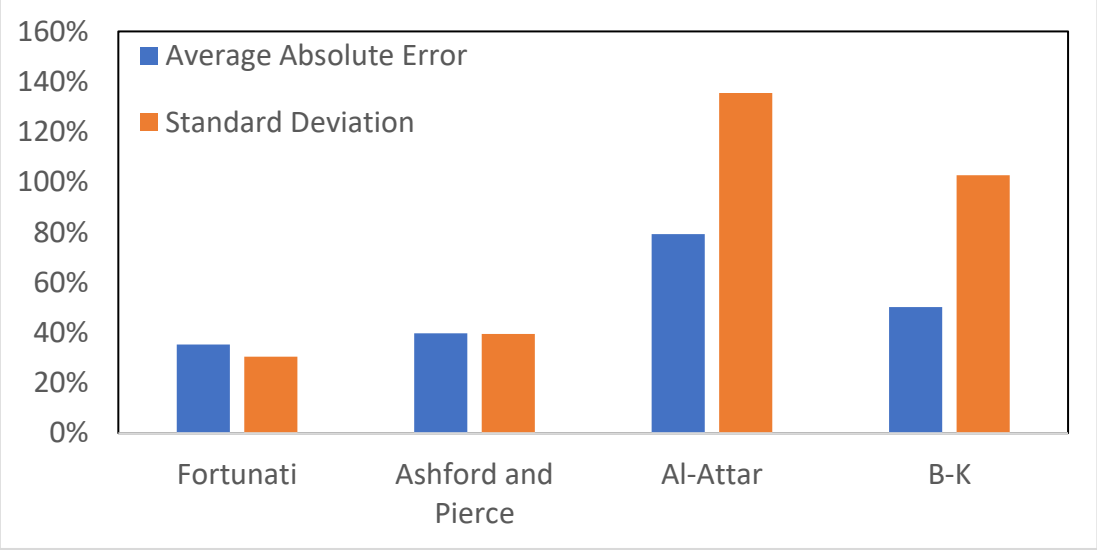

Figure 7-4: Field Performance Comparison for Correlations Studied

8 CONCLUSIONS

8.1. Conclusions

This study has evaluated three models together with two modifications on Sachdeva et al. model (1986) and four correlations for prediction of multiphase flow through choke throat. The main conclusions that can be determined out from this thesis are:

i. Models anchored in thermodynamic principles outperformed correlations.

ii. The Sachdeva et al. model, with minor modifications, outperformed those studied here. Among the correlations studied, the Fortunati correlation outperformed others.

iii. As expected, a field-specific correlation does not work well in other settings. The B-K correlation seems to overestimate flow rate.

iv. The best value of discharge coefficient for Sachdeva et al. model is 0.90 for both lab and field datasets. The best values of discharge coefficient for Simpson et al. slip correlation used on Sachdeva et al. model are 0.66 and 0.752 for lab and field datasets, respectively.

v. Though by correcting k and n for Sachdeva et al. model, the prediction performance was not improved much, this correction is recommended and should be applied theoretically;

vi. The best correlation for calculating slip ratio is the constants proposed by Simpson et al. for Grolmes and Leung equation. The best values of discharge coefficient for Simpson et al. slip correlation used on Sachdeva et al. model with k/n correction is 0.66 and 0.752 respectively for lab and field data;

vii. Considerations of slip between the gas and liquid phases at the choke-throat condition appear unimportant for improving a model's performance. This outcome is a direct consequence of the dominance of annular or mist flow, wherein the phase slippage is absent.

viii. Most flow patterns occurred at choke throat condition are annular/mist flow with negligible slip velocity. At choke throat, gas phases tend to carry liquid phases and the difference between these two phases are negligible;

ix. A rate dependent and Reynolds number dependent choke discharge coefficient can be determined. Equations for lab and field data are provided for calculation.

8.2. Future Work

The Hydro long and short model proposed by Schuller et al. (2003) should be studied and compared to other existing models to see the performance.

REFERENCES

1. Al-Attar, H. H. 2010. New Correlations for Critical and Subcritical Two-Phase Flow Through Surface Chokes in High-Rate Oil Wells. *SPE Projects, Facilities & Construction* **5** (1): 31-37. SPE-120788-PA. DOI: 10.2118/120788-PA.
2. Al-safran, E. M., & Kelkar, M. G. 2009. Predictions of Two-Phase Critical-Flow Boundary and Mass-Flow Rate Across Chokes. SPE *Prod & Oper* **24** (2): 249-256. SPE-109243-PA. DOI:10.2118/109243-PA
3. Ashford, F.E. and Pierce, P.E. 1975. Determining Multiphase Pressure Drops and Flow Capacities in Down-Hole Safety Valves. *J. Pet Tech* **27** (9): 1145-1152. SPE-5161-PA. DOI: 10.2118/5161-PA.
4. Castrup, S., Latif, F., & Al Kalbani, A. 2012. Tapered-Bean Steam Chokes Revisited. *SPE Prod & Oper* **27** (2): 205-210. SPE-144615-PA. DOI: 10.2118/144615-PA.
5. Chisholm. D. 1983. Two Phase Flow in Pipelines and Heat Exchangers, first edition. Longman Higher Education, London.
6. Fortunati, F. 1972. Two-Phase Flow through Wellhead Chokes. Presented at SPE European Spring Meeting. Amsterdam, Netherlands. 16-18 May. SPE-3742-MS. DOI: 10.2118/3742-MS.
7. Grolmes, A. M., Leung, C., 1985. J. Chemical. Engineering. Progress. 8 (p. 81).
8. Hasan A. R. and Kabir, C. S. 2002. Fluid Flow and Heat Transfer in Wellbores, first edition. Richardson, Texas: Society of Petroleum Engineers.

9. Haug. R. K. 2012. Multiphase Flow Though Chokes. MSc thesis, Norwegian University of Science and Technology, Trondheim, Norway.
10. Juliana, M and Milan, S. 2016. Improvement of Multiphase Flow Rate Model for Chokes. *Journal of Petroleum Science and Engineering* **145**: 321-327. http://dx.doi.org/10.1016/j.petrol.2016.05.022
11. Kabir, C. S. and Hasan, A. R., Simplified Wellbore Flow Modeling in Gas-Condensate Systems. Presented at SPE Annual Technical Conference and Exhibition, Houston, TX, 26-29 September 2004. SPE-89754-MS/ DOI: 10.2118/89754-MS.
12. Lateef, A. K., & Omeke, J. 2011. Specific Heat Capacity of Natural Gas; Expressed as a Function of Its Specific Gravity and Temperature. Presented at the SPE Nigeria Annual International Conference and Exhibition, Abuja, Nigeria, 30 July – 3 August. SPE-150808-MS. DOI: 10.2118/150808-MS.
13. Nasriani, H. R., & Kalantari ASL, A. 2011. Two-Phase Flow Choke Performance in High Rate Gas Condensate Wells. Presented at SPE Asia Pacific Oil and Gas Conference and Exhibition, Jakarta, Indonesia. 20-22 September. SPE-145576-MS. DOI:10.2118/145576-MS
14. Perkins, T.K. 1993. Critical and Subcritical Flow of Multiphase Mixtures Through Chokes. *SPE Drill & Compl* **8** (4):271-276. SPE-20633-PA. DOI: 10.2118/20633-PA.
15. Perry, R.H. 1950. Perry's Chemical Engineers' Handbook, third edition, 404. New York: McGraw-Hill.

16. Sachdeva, R. 1984. Two-phase flow in chokes. MSc thesis, University of Tulsa, Tulsa, Oklahoma.

17. Sachdeva, R., Schmidt, Z., Brill, J.P. and Blais, R.M., Two-Phase Flow Through Chokes. Presented at the SPE Annual Technical Conference and Exhibition, New Orleans, LA, 5-8 October 1986. SPE-15657-MS. DOI: 10.2118/15657-MS.

18. Safar Beiranvand, M., & Babaei Khorzoughi, M. 2012. Introducing a New Correlation for Multiphase Flow Through Surface Chokes With Newly Incorporated Parameters. *SPE Prod & Oper* **27** (4): 422-428. SPE-158649-PA. DOI:10.2118/158649-PA

19. Schüller, R.B., Munaweera, S., Selmer-Olsen, S., and Solbakken, T. 2006. Critical and Subcritical Oil/Gas/Water Mass-flow Rate Experiments and Predictions for Chokes. *SPE Prod & Oper* **21** (3): 372-380. SPE-88813-PA. DOI: 10.2118/88813-PA.

20. Schüller, R.B., Solbakken, T., and Selmer-Olsen, S. 2003. Evaluation of Multiphase Flow Rate Models for Chokes Under Subcritical Oil/Gas/Water Flow Conditions. *SPE Prod & Fac* **18** (3): 170-181. SPE-84961-PA. DOI: 10.2118/84961-PA.

21. S. Rastoin, Z. Schmidt and D. R. Doty. 1997. A Review of Multiphase Flow Through Chokes. ASME J. Energy Resour. Technol **119** (1): 1-10. DOI:10.1115/1.2794216.

APPENDIX A

MATHEMATICAL DERIVATION OF AVERAGE DENSITY EQUATIONS

Expression of two-phase mixture density:

Starting with the original equation for mixture density:

$$\rho_m = \alpha\rho_g + (1-\alpha)\rho_l \qquad \text{A-1}$$

If using mass fractions to replace void fraction which makes it easier to use for choke models, first use void fraction to express mass flux rate:

$$\dot{m}_g = x_g\dot{m}_{g+l} = \alpha\times A\times V_g\times\rho_g \qquad \text{A-2}$$

$$\dot{m}_l = x_l\dot{m}_{g+l} = (1-\alpha)\times A\times V_l\times\rho_l \qquad \text{A-3}$$

If combing equations A-2 and A-3 and solve for void fraction, void fraction can be expressed by using mass fraction items:

$$\alpha = \frac{x_g\rho_l}{\frac{V_g}{V_l}x_l\rho_g + x_g\rho_l} \qquad \text{A-4}$$

By substituting expression of void fraction Equation A-4 into Equation A-1, the mixture density equation with mass fraction can be derived:

$$\rho_m = \frac{\rho_g\rho_l(x_g + \frac{V_g}{V_l}x_l)}{x_g\rho_l + \frac{V_g}{V_l}x_l\rho_g} \qquad \text{A-5}$$

where the velocity ratio can then be expressed as slip ratio: S, and the final version of equation will be:

$$\rho_m = \frac{\rho_g\rho_l(x_g + Sx_l)}{x_g\rho_l + Sx_l\rho_g} \qquad \text{A-6}$$

If there is no slippage effect, then S equals to 1, the above equation can then be simplified to homogeneous density equation as sum of gas and liquid mass fraction equals to 1:

$$\rho_m = \frac{\rho_g \rho_l}{x_g \rho_l + x_l \rho_g} \quad \text{A-7}$$

Expression of momentum density:

Starting from the definition of momentum flux, which is the momentum flow rate per area, momentum flow rate can be calculated by multiplying mass flow rate and flow velocity. Hence, for a multiphase flow:

$$\text{momentum flux} = \frac{(\dot{m}_g + \dot{m}_l)V}{A} = \frac{(\dot{m}_g + \dot{m}_l)(x_g V_g + x_l V_l)}{A} \quad \text{A-8}$$

By substituting the phase velocity parts of Equation A-2 and Equation A-3 into Equation A-8, and then substitute Equation A-4 to replace the void fraction, the following expression is derived:

$$V_g = \frac{\dot{m}_g}{\alpha A \rho_g} = \frac{\dot{m}_g (S x_l \rho_g + x_g \rho_l)}{x_g \rho_l A \rho_g} \quad \text{A-9}$$

$$V_l = \frac{\dot{m}_g}{(1-\alpha) A \rho_g} = \frac{\dot{m}_l (S x_l \rho_g + x_g \rho_l)}{S x_l \rho_l A \rho_g} \quad \text{A-10}$$

$$\text{momentum flux} = \frac{(\dot{m}_g + \dot{m}_l)}{A} \frac{S x_l \rho_g + x_g \rho_l}{\rho_g A \rho_l} (\dot{m}_g + \frac{\dot{m}_l}{S}) \quad \text{A-11}$$

Because mass flow rate for individual phase can be expressed as total mass flow rate multiplied by mass fraction of that phase, so:

$$\text{momentum flux} = \frac{(\dot{m}_g + \dot{m}_l)^2}{A^2} \frac{S x_l \rho_g + x_g \rho_l}{\rho_g \rho_l} (x_g + \frac{x_l}{S}) \quad \text{A-12}$$

Then express momentum flux with density variable:

$$\text{momentum flux} = \frac{(\dot{m}_g + \dot{m}_l)V}{A} = \left(\frac{\dot{m}_g + \dot{m}_l}{A}\right)^2 \frac{1}{\rho_e} \quad \text{A-13}$$

Connect Equation A-12 and A-13:

$$\frac{1}{\rho_e} = \frac{S x_l \rho_g + x_g \rho_l}{\rho_g \rho_l} (x_g + \frac{x_l}{S}) \quad \text{A-14}$$

As can be seen, if assuming no slippage effect, then momentum density is simplified to homogeneous density.

APPENDIX B

ERRORS AND TYPOS OF EXISTING MODELS AND CORRELATIONS

During evaluating selected choke models and correlations, some errors and typos were detected. The errors are listed in this appendix to help avoid making such errors:

Errors of Juliana. M and Milan. S model (2016):

Juliana. M and Milan. S (2016) used Equation A-42 of their original paper to calculate final mass flow rate. However, a bracket is missing which can cause incorrect calculation. The correct equation is:

$$\dot{m}_4 = \left\{2\rho_m^2 p_1 \left[x_g + \frac{1-x_g}{R}\right]\left[R\left(1-x_g\right)v_l(1-y) + \frac{kx_g}{k-1}\left(v_{g1} - yv_{g4}\right)\right]\right\}^{0.5} \quad \text{B - 1}$$

Errors of Al-Safran and Kelkar model (2009):

Al-Safran and Kelkar (2009) used Equation (4) of their original paper to calculate final mass flow rate. There is a constant C used in this equation to represent for discharge coefficient. Al-Safran and Kelkar (2009) further suggests that $C = 2{,}000C_D^2$ should be used for SI units and $C = 2C_D^2 \times g_c \times 144$ should be used for customary units. However, from the derivation the correct equation for SI unit should be $C = 2C_D^2$.

Errors of Sachdeva et. al model (1986):

Sachdeva et al. (1986) used Equation (2) and Equation (4) of their original paper to estimate flow boundary and mass flow rate. However, from the model derivation, Al-Safran and Kelkar (2009) pointed out that the specific heat capacity k should be replaced by polytropic coefficient n.

APPENDIX C

EXAMPLE IMPLEMENTATION OF FLOW BOUNDARY DETERMINATION FOR AF-SAFRAN AND KELKAR MODEL (2009)

During evaluating Al-Safran and Kelkar model (2009), an inconsistency was found for Equation **(38)** which is used to determine flow boundary between critical and subcritical flow. As illustrated, this equation requires the use of slip ratio which depends on flow boundary results first. Therefore, a circular calculation can be caused when evaluating flow boundary. Following shows an example about how this inconsistency during evaluating flow boundary for Al-Safran and Kelkar model (2009) is solved in this study:

i. For each data point, two different flow boundary critical pressure ratio values are computed by using critical and subcritical slip ratio separately. Name these two values $yc_{critical}$ and $yc_{subcritical}$ respectively.

ii. The actual pressure ratio ($\frac{p_4}{p_1}: y_{actual}$) is calculated to compare with $yc_{critical}$ and $yc_{subcritical}$;

iii. If $y_{actual} < yc_{critical}$ and $y_{actual} < yc_{subcritical}$ happen simultaneously, then there is no question that flow is critical flow;

iv. If $y_{actual} > yc_{critical}$ and $y_{actual} > yc_{subcritical}$ happen simultaneously, then there is no question that flow is subcritical flow;

v. However, for situations such as: $y_{actual} < yc_{critical}$ and $y_{actual} > yc_{subcritical}$ or $y_{actual} > yc_{critical}$ and $y_{actual} < yc_{subcritical}$, it is not clear what flow regime it is.

In such situations, both critical and subcritical mass flow rate are calculated and interpolation method is used to compute final mass flow rate in this study.

APPENDIX D

MATHEMATICAL DERIVATION OF SACHDEVA MODEL WITH K/N CORRECTION AND SLIPPAGE EFFECT

The momentum mixture density discussed in APPENDIX A:

$$\rho_m = \frac{\rho_g \rho_l (x_g + S x_l)}{x_g \rho_l + S x_l \rho_g} \qquad \text{D - 1}$$

The mixture specific volume at choke throat condition:

$$v_{m2} = \left[x_{g2} v_{g2} + S(1 - x_{g2}) v_l\right]\left[x_{g2} + \frac{1}{S}(1 - x_{g2})\right] \qquad \text{D - 2}$$

The final mass flow rate at choke throat condition:

$$\dot{m}_2 = C_D A_2 \left\{ 2\rho_{m2}^2 p_1 \left(x_g + \frac{1 - x_g}{S}\right)\left[S(1 - x_g) v_l (1 - y) + \frac{n x_g}{n - 1}\left(v_{g1} - y v_{g2}\right)\right]\right\}^{0.5} \qquad \text{D - 3}$$

The expression for defining critical/subcritical flow boundary:

$$y = \left\{ \frac{\frac{n}{n-1} + \frac{S(1 - x_g) v_l (1 - y)}{x_g v_{g1}}}{\frac{n}{n-1} + \frac{n}{2} + \frac{nS(1 - x_g) v_l}{x_g v_{g2}} + \frac{n}{2}\left(\frac{S(1 - x_g) v_l}{x_g v_{g2}}\right)^2} \right\}^{0.5} \qquad \text{D - 4}$$

APPENDIX E

DATA POINTS USED TO DRAW FLOW BOUNDARY DIAGRAM FOR

FORTUNATI CORRELATION

Left Boundary		Right Boundary		β=1		β=0.98	
Mixture Velocity (m/sec)	P2/P1	Mixture Velocity (m/sec)	P2/P1	Mixture Velocity (m/sec)	P2/P1	Mixture Velocity (m/sec)	P2/P1
293	0.5	293	0	293	0	165.555555	0
268	0.48888	293	0.1	293	0.1	165.555555	0.1
230	0.4777	293	0.2	293	0.2	165.555555	0.2
190	0.4611	293	0.225	293	0.225	165.555555	0.225
170	0.45	293	0.25	293	0.25	165.555555	0.25
150	0.4389	293	0.275	293	0.275	165.555555	0.275
128.5	0.423	293	0.3	293	0.3	165.555555	0.3
100	0.4	293	0.325	293	0.325	165.555555	0.325
90	0.3889	293	0.35	293	0.35	165.555555	0.35
70	0.35	293	0.375	293	0.375	165.555555	0.375
52.22	0.3	293	0.4	293	0.4	165.555555	0.4
40	0.25	293	0.425	293	0.425	165.555555	0.444444
28.89	0.2	293	0.45	293	0.45	158	0.45
17.78	0.15	293	0.475	293	0.475	142	0.475
		293	0.5	293	0.5	132	0.5
		280	0.525	280	0.525	125	0.525
		270	0.55	270	0.55	117	0.55
		258	0.575	258	0.575	111	0.575
		250	0.6	250	0.6	106	0.6
		240	0.625	240	0.625	101	0.625
		230	0.65	230	0.65	95	0.65
		220	0.675	220	0.675	93	0.675
		210	0.7	210	0.7	88	0.7
		198	0.725	198	0.725	84	0.725
		189	0.75	189	0.75	78	0.75
		177	0.775	177	0.775	73	0.775
		167	0.8	167	0.8	68	0.8
		156	0.825	156	0.825	64	0.825
		143	0.85	143	0.85	57	0.85

		128	0.875	128	0.875	51	0.875
		112	0.9	112	0.9	45	0.9
		95	0.925	95	0.925	36	0.925
		76	0.95	76	0.95	27	0.95
		45	0.975	45	0.975	15	0.975
		0	1	0	1	0	1

β=0.95		β=0.90		β=0.80		β=0.70	
Mixture Velocity (m/sec)	P2/P1	Mixture Velocity (m/sec)	P2/P1	Mixture Velocity (m/sec)	P2/P1	Mixture Velocity (m/sec)	P2/P1
115.55555	0	85.55556	0	62.5	0	48	0
115.55555	0.1	85.55556	0.1	62.5	0.1	48	0.1
115.55555	0.2	85.55556	0.2	62.5	0.2	48	0.2
115.55555	0.225	85.55556	0.225	62.5	0.225	48	0.225
115.55555	0.25	85.55556	0.25	62.5	0.25	48	0.25
115.55555	0.275	85.55556	0.275	62.5	0.275	48	0.275
115.55555	0.3	85.55556	0.3	62.5	0.3	48	0.2833
115.55555	0.325	85.55556	0.325	62.5	0.325	47	0.3
115.55555	0.35	85.55556	0.35	62.5	0.32778	45	0.325
115.55555	0.375	85.55556	0.375	58	0.35	43	0.35
115.55555	0.4	85.55556	0.37778	54	0.375	40	0.375
115.55555	0.4133	80	0.4	51	0.4	37	0.4
110	0.425	76	0.425	48	0.425	35	0.425
102	0.45	72	0.45	46	0.45	34.5	0.45
95	0.475	68	0.475	44	0.475	32	0.475
90	0.5	65	0.5	42	0.5	30	0.5
85	0.525	61	0.525	40	0.525	28	0.525
78	0.55	57	0.55	38	0.55	26.5	0.55
74	0.575	55	0.575	37	0.575	26	0.575
71	0.6	52	0.6	36	0.6	25	0.6
67	0.625	49	0.625	35	0.625	24	0.625
63	0.65	47	0.65	34	0.65	23	0.65
60	0.675	45	0.675	33	0.675	22	0.675
57	0.7	43	0.7	32	0.7	21	0.7
55	0.725	40	0.725	31	0.725	20	0.725
52	0.75	38	0.75	29	0.75	18	0.75
49	0.775	36	0.775	27	0.775	17	0.775
47	0.8	33	0.8	26	0.8	16	0.8

44	0.825	31	0.825	24	0.825	15	0.825
39	0.85	27	0.85	21	0.85	14	0.85
35	0.875	24	0.875	18	0.875	13	0.875
30	0.9	20	0.9	16	0.9	11	0.9
25	0.925	16	0.925	13	0.925	8	0.925
18	0.95	12	0.95	10	0.95	6	0.95
10	0.975	6	0.975	6	0.975	3	0.975
0	1	0	1	0	1	0	1

β=0.60		β=0.50		β=0.40		β=0.00	
Mixture Velocity (m/sec)	P2/P1	Mixture Velocity (m/sec)	P2/P1	Mixture Velocity (m/sec)	P2/P1	Mixture Velocity (m/sec)	P2/P1
42.35294	0	36	0	32.5	0	22.5	0.177778
42.35294	0.1	36	0.1	32.5	0.1	15.5556	0.3
42.35294	0.2	36	0.2	32.5	0.2	12.2222	0.4
42.35294	0.225	36	0.225	32.5	0.225	10.1	0.5
42.35294	0.25	36	0.23978	28	0.25	9.5	0.6
42.35294	0.2588	34	0.25	26	0.275	8.4444	0.7
40	0.275	32	0.275	24	0.3	6.6667	0.8
38	0.3	30	0.3	22.5	0.325	4.4444	0.9
36	0.325	28	0.325	20.5	0.35	2.2222	0.95
34	0.35	26	0.35	19	0.375	0	1
32	0.375	24	0.375	17.5	0.4		
30	0.4	23.5	0.4	16.5	0.425		
28	0.425	21	0.425	16	0.45		
26.5	0.45	19	0.45	14.5	0.475		
25	0.475	18	0.475	13.5	0.5		
24	0.5	17	0.5	13	0.525		
23	0.525	16	0.525	12.5	0.55		
22	0.55	15.5	0.55	12	0.575		
20.5	0.575	15	0.575	12	0.6		
19	0.6	14	0.6	12	0.625		
18	0.625	13	0.625	11.5	0.65		
17.5	0.65	12	0.65	11	0.675		
16.5	0.675	11	0.675	10	0.7		
16	0.7	11	0.7	10	0.725		
15	0.725	10.5	0.725	10	0.75		

14	0.75	10	0.75	9	0.775		
13	0.775	10	0.775	8	0.8		
12	0.8	9.5	0.8	7	0.825		
11	0.825	9.5	0.825	6.5	0.85		
10.5	0.85	9	0.85	6.5	0.875		
10	0.875	8	0.875	6	0.9		
7.5	0.9	7	0.9	5	0.925		
7	0.925	6	0.925	3	0.95		
5	0.95	5	0.95	2	0.975		
2.5	0.975	2.5	0.975	0	1		

```
Public Function fortunati_subcritical(pratio, beta) As Double
    If beta = 1 Then
        A7 = -2.69637 * 10 ^ (5)
        A6 = 1.15490610651 * 10 ^ (6)
        A5 = -2.041026029 * 10 ^ (6)
        A4 = 1.903067032 * 10 ^ (6)
        A3 = -9.865524698772 * 10 ^ (5)
        A2 = 2.69022749147 * 10 ^ (5)
        A1 = -2.9777646 * 10 ^ (4)
        v = A7 * pratio ^ 6 + A6 * pratio ^ 5 + A5 * pratio ^ 4 + A4 * pratio ^ 3 + A3 * pratio ^ 2 + A2 * pratio + A1
    ElseIf beta = 0.98 Then
        A4 = -1805.6
        A3 = 3872.3
        A2 = -2918.8
        A1 = 852.81
        v = A4 * pratio ^ 3 + A3 * pratio ^ 2 + A2 * pratio + A1
    ElseIf beta > 0.98 And beta < 1 Then
        A4 = -1805.6
        A3 = 3872.3
        A2 = -2918.8
        A1 = 852.81
        vlow = A4 * pratio ^ 3 + A3 * pratio ^ 2 + A2 * pratio + A1
        B7 = -2.69637 * 10 ^ (5)
        B6 = 1.15490610651 * 10 ^ (6)
        B5 = -2.041026029 * 10 ^ (6)
        B4 = 1.903067032 * 10 ^ (6)
        B3 = -9.865524698772 * 10 ^ (5)
        B2 = 2.69022749147 * 10 ^ (5)
        B1 = -2.9777646 * 10 ^ (4)
        vhigh = B7 * pratio ^ 6 + B6 * pratio ^ 5 + B5 * pratio ^ 4 + B4 * pratio ^ 3 + B3 * pratio ^ 2 + B2 * pratio + B1
        v = (beta - 0.98) * (vhigh - vlow) / (1 - 0.98) + vlow
    ElseIf beta = 0.95 Then
        A4 = -976.55
        A3 = 2064.4
        A2 = -1565.3
        A1 = 478.35
        v = A4 * pratio ^ 3 + A3 * pratio ^ 2 + A2 * pratio + A1
    ElseIf beta > 0.95 And beta < 0.98 Then
        A4 = -976.55
        A3 = 2064.4
        A2 = -1565.3
        A1 = 478.35
        vlow = A4 * pratio ^ 3 + A3 * pratio ^ 2 + A2 * pratio + A1
        B4 = -1805.6
        B3 = 3872.3
        B2 = -2918.8
        B1 = 852.81
        vhigh = B4 * pratio ^ 3 + B3 * pratio ^ 2 + B2 * pratio + B1
        v = (beta - 0.95) * (vhigh - vlow) / (0.98 - 0.95) + vlow
```

```
ElseIf beta = 0.9 Then
    A4 = -447.4557
    A3 = 911.23
    A2 = -712.7577
    A1 = 249.0164
    v = A4 * pratio ^ 3 + A3 * pratio ^ 2 + A2 * pratio + A1
ElseIf beta > 0.9 And beta < 0.95 Then
    A4 = -447.4557
    A3 = 911.23
    A2 = -712.7577
    A1 = 249.0164
    vlow = A4 * pratio ^ 3 + A3 * pratio ^ 2 + A2 * pratio + A1
    B4 = -976.55
    B3 = 2064.4
    B2 = -1565.3
    B1 = 478.35
    vhigh = B4 * pratio ^ 3 + B3 * pratio ^ 2 + B2 * pratio + B1
    v = (beta - 0.9) * (vhigh - vlow) / (0.95 - 0.9) + vlow
ElseIf beta = 0.8 Then
    A5 = 172.435619
    A4 = -844.051095
    A3 = 1186.073347
    A2 = -709.192979
    A1 = 195.284225
    v = A5 * pratio ^ 4 + A4 * pratio ^ 3 + A3 * pratio ^ 2 + A2 * pratio + A1
ElseIf beta > 0.8 And beta < 0.9 Then
    A5 = 172.435619
    A4 = -844.051095
    A3 = 1186.073347
    A2 = -709.192979
    A1 = 195.284225
    vlow = A5 * pratio ^ 4 + A4 * pratio ^ 3 + A3 * pratio ^ 2 + A2 * pratio + A1
    B4 = -447.4557
    B3 = 911.23
    B2 = -712.7577
    B1 = 249.0164
    vhigh = B4 * pratio ^ 3 + B3 * pratio ^ 2 + B2 * pratio + B1
    v = (beta - 0.8) * (vhigh - vlow) / (0.9 - 0.8) + vlow
ElseIf beta = 0.7 Then
    A5 = -184.700835
    A4 = 268.652689
    A3 = -18.214971
    A2 = -155.097956
    A1 = 89.910413
    v = A5 * pratio ^ 4 + A4 * pratio ^ 3 + A3 * pratio ^ 2 + A2 * pratio + A1
ElseIf beta > 0.7 And beta < 0.8 Then
    A5 = -184.700835
    A4 = 268.652689
    A3 = -18.214971
    A2 = -155.097956
    A1 = 89.910413
    vlow = A5 * pratio ^ 4 + A4 * pratio ^ 3 + A3 * pratio ^ 2 + A2 * pratio + A1
    B5 = 172.435619
    B4 = -844.051095
    B3 = 1186.073347
    B2 = -709.192979
    B1 = 195.284225
    vhigh = B5 * pratio ^ 4 + B4 * pratio ^ 3 + B3 * pratio ^ 2 + B2 * pratio + B1
    v = (beta - 0.7) * (vhigh - vlow) / (0.8 - 0.7) + vlow
ElseIf beta = 0.6 Then
    A5 = -187.508783
    A4 = 302.360081
    A3 = -71.380227
    A2 = -115.429019
    A1 = 72.31816
    v = A5 * pratio ^ 4 + A4 * pratio ^ 3 + A3 * pratio ^ 2 + A2 * pratio + A1
ElseIf beta > 0.6 And beta < 0.7 Then
    A5 = -187.508783
    A4 = 302.360081
    A3 = -71.380227
    A2 = -115.429019
    A1 = 72.31816
    vlow = A5 * pratio ^ 4 + A4 * pratio ^ 3 + A3 * pratio ^ 2 + A2 * pratio + A1
    B5 = -184.700835
    B4 = 268.652689
    B3 = -18.214971
    B2 = -155.097956
    B1 = 89.910413
    vhigh = B5 * pratio ^ 4 + B4 * pratio ^ 3 + B3 * pratio ^ 2 + B2 * pratio + B1
    v = (beta - 0.6) * (vhigh - vlow) / (0.7 - 0.6) + vlow
```

```
ElseIf beta > 0.5 And beta < 0.6 Then
    A5 = -218.323956
    A4 = 394.624799
    A3 = -165.946314
    A2 = -65.55094
    A1 = 55.249112
    vlow = A5 * pratio ^ 4 + A4 * pratio ^ 3 + A3 * pratio ^ 2 + A2 * pratio + A1
    B5 = -187.508783
    B4 = 302.360081
    B3 = -71.380227
    B2 = -115.429019
    B1 = 72.31816
    vhigh = B5 * pratio ^ 4 + B4 * pratio ^ 3 + B3 * pratio ^ 2 + B2 * pratio + B1
    v = (beta - 0.5) * (vhigh - vlow) / (0.6 - 0.5) + vlow
ElseIf beta = 0.4 Then
    A5 = -27.459612
    A4 = -110.39557
    A3 = 298.961091
    A2 = -229.97951
    A1 = 68.916089
    v = A5 * pratio ^ 4 + A4 * pratio ^ 3 + A3 * pratio ^ 2 + A2 * pratio + A1
ElseIf beta > 0.4 And beta < 0.5 Then
    A5 = -27.459612
    A4 = -110.39557
    A3 = 298.961091
    A2 = -229.97951
    A1 = 68.916089
    vlow = A5 * pratio ^ 4 + A4 * pratio ^ 3 + A3 * pratio ^ 2 + A2 * pratio + A1
    B5 = -218.323956
    B4 = 394.624799
    B3 = -165.946314
    B2 = -65.55094
    B1 = 55.249112
    vhigh = B5 * pratio ^ 4 + B4 * pratio ^ 3 + B3 * pratio ^ 2 + B2 * pratio + B1
    v = (beta - 0.4) * (vhigh - vlow) / (0.5 - 0.4) + vlow
ElseIf beta = 0 Then
    A5 = 11.9501
    A4 = -136.360736
    A3 = 224.909909
    A2 = -141.947109
    A1 = 41.40624
    v = A5 * pratio ^ 4 + A4 * pratio ^ 3 + A3 * pratio ^ 2 + A2 * pratio + A1
    ElseIf beta > 0 And beta < 0.4 Then
        A5 = 11.9501
        A4 = -136.360736
        A3 = 224.909909
        A2 = -141.947109
        A1 = 41.40624
        vlow = A5 * pratio ^ 4 + A4 * pratio ^ 3 + A3 * pratio ^ 2 + A2 * pratio + A1
        B5 = -27.459612
        B4 = -110.39557
        B3 = 298.961091
        B2 = -229.97951
        B1 = 68.916089
        vhigh = B5 * pratio ^ 4 + B4 * pratio ^ 3 + B3 * pratio ^ 2 + B2 * pratio + B1
        v = (beta - 0) * (vhigh - vlow) / (0.4 - 0) + vlow
    End If
    fortunati_subcritical = v
End Function
```